

Reactive Extrusion Process for Maleic Anhydride Functionalization of Polypropylene and its Applications as Compatibilizer to Develop PET Blends



Name: Asra Tariq

Reg. No: 00000117414

**This thesis is submitted as a partial fulfillment of the requirements for
the degree of**

MS in Materials and Surface Engineering

Supervisor Name: Dr. Nasir Mehmood Ahmad

**School of Chemical and Materials Engineering (SCME)
National University of Sciences and Technology (NUST), H-12
Islamabad, Pakistan**

October, 2017

I dedicate this thesis to my parents and teachers for their immense support, encouragement and motivation.

Acknowledgements

All praise is for **Allah Almighty**, the most gracious and the most beneficent, Who has always helped me in every step of my life and bestowed me with His blessings Alhumdulilah. All esteem and reverence for his **Holy Prophet Muhammad (peace be upon him)** who has enabled us to shape our lives according to the teachings of Islam.

I am much thankful to my parents and siblings for their love, affection and support. They encouraged me and prayed for me. All I am is because of my family. May Allah keep them in His mercy and protection.

I would like to express my sincere gratitude to my thesis supervisor, Dr. Nasir Mehmood Ahmad for his guidance, encouragement and continuous support. His patience, motivation and immense knowledge helped me all the time of research work and writing of this thesis. I cannot imagine a better supervisor and mentor.

I would also like to thank to my committee members, Dr. Zakir Hussain (SCME) and Dr. Muhammad Nabeel Anwar (SMME) for supporting in project and thesis writing. Without their participation and input, the research work could not have been successfully conducted. I am much grateful to my all teachers who built my knowledge and educate me.

I would also like to acknowledge Dr. Zulfiqar Ali of Department of Chemical Engineering at COMSATS Institute of Information Technology Lahore for his guidance and help in experimental part of research by providing laboratory facility. I am highly grateful to industries, Astrofilms, Packages, Gatron and Tripack for providing materials and cooperating with me in my application of thesis.

I am highly gratified to my class fellow Naveed Ahmad and my friends Nadia Siyal and Rishi Naeem for encouraging me and always supporting me. At the end I would like to thanks all the staff at School of Chemical and Materials Engineering, NUST, Islamabad for cooperating with me during my work.

Table of Contents

Chapter 1: Introduction	3
1.1: Polymer Blends.....	3
1.2: Reactive Extrusion.....	5
1.3: Plastics based Food Packaging	6
1.4: Polymers Permeability	9
1.4: Research Objectives.....	13
Chapter 2: Literature Survey	15
2.1: Barrier Properties of Polymer Films and Functionalized Food Packaging Films.....	15
2.2: Polymer Blends in Food Packaging.....	20
2.3: Grafting of Polyolefin.....	22
Chapter 3: Experimental Procedures	24
3a: Preparation and Characterization of Functionalized Polypropylene	24
3a.1: Materials and Methods	24
3a.2: Characterization of Grafted PP Samples.....	29
3b: Fabrication of Polyethylene Terephthalate (PET) and Polypropylene (PP) blends' films	31
3b.1: Materials and Methods.....	31
3b.2: Preparation of Blends.....	31
3b.3: Preparation of Polymer Blends' Film	31
3b.4: Characterization of Polymer Blends	31
3b.4.1: Fourier Transform Infrared Spectroscopy (FTIR)	32
3b.4.2: Differential Scanning Calorimetry (DSC)	32
3b.4.3: Scanning Electron Microscope (SEM)	33

3b.4.4: Films' Water Permeability	33
Chapter 4: Results and Discussion.....	34
4a: Results and Discussion of Grafted samples	34
4a.1: Torque Evolution of Grafted Polypropylene in Internal Mixer	34
4a.2: FTIR Analysis of Grafted PP Samples.....	39
4a.3: Thermal Analysis of Grafted Samples	44
4b: Results and Discussion of Blended Films	48
4b.1: Fourier Transform Infrared Spectroscopy (FTIR)	48
4b.2: Thermal Analysis by Differential Scanning Calorimetry (DSC).....	49
4b.3: Morphology by Scanning Electron Microscopy (SEM)	52
4b.4: Water vapours Permeability.....	55
Conclusion.....	58
References.....	60

LIST OF FIGURES

Figure 1.1: Phase diagrams showing A) LCST and B) UCST for polymer blends	4
Figure 1.2: Permeation of a substance through a plastic packaging material	10
Figure 2.1: Structure of Montmorillonite Clay	16
Figure 2.2: Effect of Clay's dispersion on the tortuosity of films a) random disorient clay in film b) highly oriented well dispersed clays offers high tortuosity.	17
Figure 2.3: Transmission of gas molecules through oxide coatings	19
Figure 3.1: HAAKE PolyLab OS internal engineering mixer system.	26
Figure 3.2: Simplified inside 2D view of HAAKE PolyLab OS internal mixer system	26
Figure 4.2: Measurement curves generated by HAAKE Polysoft Software for samples having MAH variation at constant BPO.	35
Figure 4.3: Effect on torque by varying MAH content at constant BPO.....	36
Figure 4.4: Effect on torque by varying BPO content at constant MAH.....	37
Figure 4.5: Torque variation by altering MAH concentration.	38
Figure 4.6: Torque variation by altering BPO concentration.....	38

Figure 4.7: FTIR analysis spectra of MAH grafted PP samples by varying MAH content (from 1 to 5) in comparison of pure PP spectra.	41
Figure 4.8: FTIR analysis spectra of MAH grafted PP samples by varying BPO content (from 1 to 5) in comparison of pure PP spectra.	43
Figure 4.9: Differential scanning calorimetry (DSC) thermograms for MAH grafted PP samples for varying MAH contents.	44
Figure 4.10: Differential scanning calorimetry (DSC) thermograms for MAH grafted PP samples for varying BPO contents.	45
Figure 4.11: Effect on percentage crystallinity for grafted samples by varying MAH and BPO content.	45
Figure 4.12: Effect on Melting Temperature (T_m) for grafted samples by varying MAH and BPO contents.	46
Figure 4.13: Melt Flow Index of functionalized samples by varying MAH and BPO ...	47
Figure 4.14: FTIR spectra comparison between pure PP, pure PET and MAH-g-PP/PP/PET.	48
Figure 4.15: DSC thermogram of MAH-g-PP/PP/PET blend, PP and PET	49
Figure 4.16: DSC thermogram of /PP/PET blend, PP and PET	50
Figure 4.17: Percentage crystallinity of blends of different composition.....	51
Figure 4.19: SEM images of 1) PP/PET and 2) MAH-g-PP/PP/PET blends with composition 40/60 and 2.5/37.5/60 respectively.	52
Figure 4.20: SEM images of 1) MAH-g-PP/PP/PET and 2) MAH-g-PP/PP/PET blends with composition 2.5/39/60 and 5/35/60 respectively.	53
Figure 4.21: SEM images of 1) MAH-g-PP/PP/PET and 2) MAH-g-PP/PP/PET blends with composition 1/39/60 and 2.5/37.5/60 respectively.	53
Figure 4.22: SEM images of fracture analysis of 60 % PET 1) 2.5% MAH-g-PP/PP/PET blends 2) 5% MAH-g-PP/PET blends 3) noncompatibilized PP/PET.....	54
Figure 4.23: Water vapours weight loss of prepared films.	55
Figure 4.24: Water vapours permeability of prepared films.	56

LIST OF TABLES

Table 1.1: Values of water permeability and oxygen permeability of various commercial plastic used in Packaging	12
Table 3.1: Experimental design by varying Maleic anhydride and constant BPO	25
Table 3.2: Experimental design by varying Benzoyl Peroxide and constant MAH	25
Table 3.3: CI values of all grafted samples	39
Table 3.4: Melt Flow Index for all processed samples and pure polypropylene.	47
Table 4.1: Composition details of PP/ PET blends	31
Table 4.2: Percentage crystallinity of PET in the blend.....	51

LIST of ABBREVIATIONS

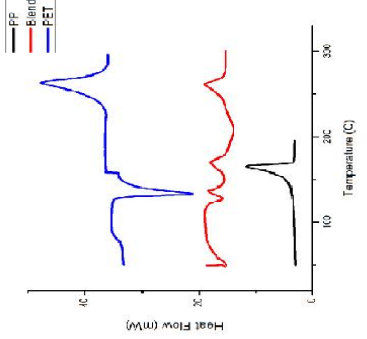
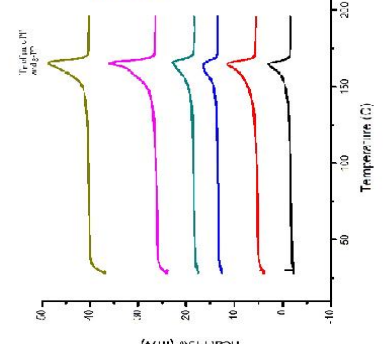
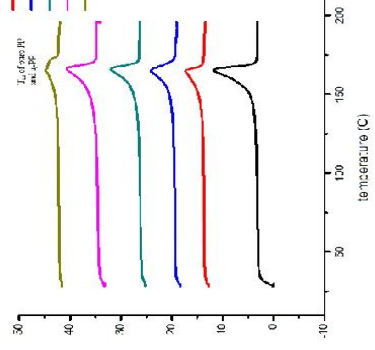
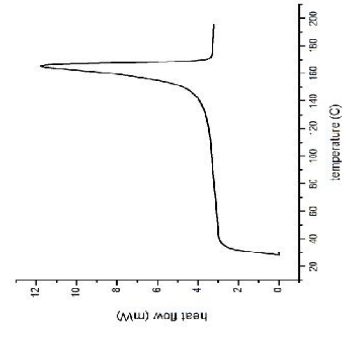
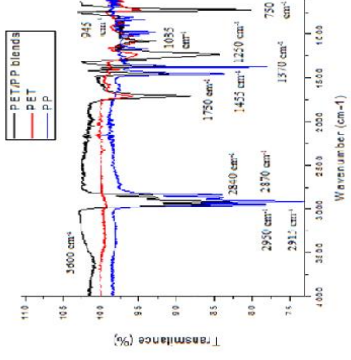
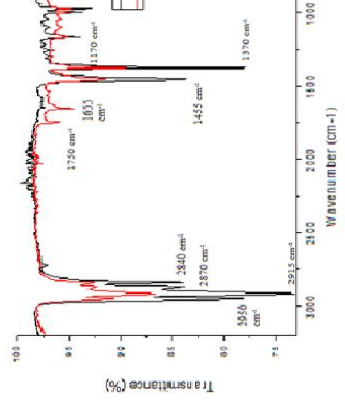
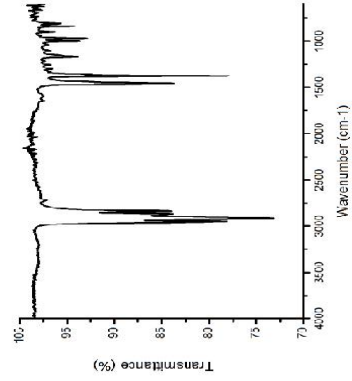
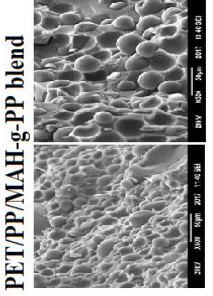
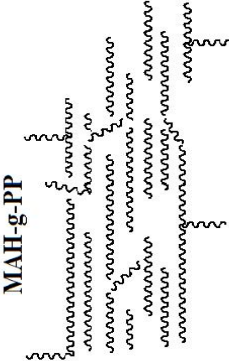
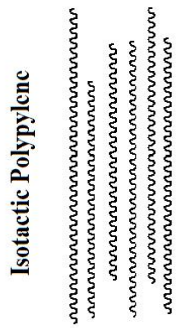
PP	Polypropylene
MAH	Maleic anhydride
BPO	Benzoyl peroxide
PET	Polyethylene terephthalate
MAH-g-PP	Maleic anhydride grafted polypropylene
LCST	Lower critical solution temperature
UCST	Upper critical solution temperature
UV	Ultra Violet
HDPE	High density polyethylene
LDPE	Low density polyethylene
PA6	Polyamide 6
SAN	Styrene acrylonitrile
ABS	Acrylonitrile butadiene styrene
PS	Polystyrene
RH	Relative humidity
PVC	Polyvinyl chloride
MMT	Montmorillonite
VDAC	vinylbenzyl dimethyl dodecyl ammonium chloride
PVD	Physical vapour deposition
BOPP	Biaxially oriented polypropylene
ALD	Atomic layer deposition
PEN	Polyethylene naphthalate
CVD	Chemical vapour deposition
WVTR	Water vapour transmission rate
OTR	Oxygen gas transmission rate
PLA	Poly lactic acid
PBS	Polybutylene succinate
SEBS	Styrene ethylene butylene styrene

POE	Polyoxyethylene
SCA	Silane coupling agent
ASTM	American society for testing and materials
DCP	Dicumyl peroxide
PP-g-AA	Acrylic acid grafted polypropylene
EVOH	Ethylene vinyl alcohol
FTIR	Fourier transform infrared spectroscopy
SEM	Scanning electron microscopy
DSC	Differential scanning calorimetry
MFI	Melt flow index
CI	Carbonyl index

ABSTRACT

Properties of polyethylene terephthalate (PET) and polypropylene (PP) can be enhanced by blending both in a specific proportion to get combined superior properties. To make a homogeneous blend, functionalization of PP can be done by grafting a required functional group on the main chain. Grafting of PP was done at varied concentration of MAH and BPO and its effect on the viscosity during and after the reaction was studied by torque rheometer and melt flow index. Functionalization of PP by free radical polymerization influenced its molecular weight owing to its chains breakage which was analysed by viscosity decrease during the reaction. At high percentage of grafting, lower molecular weight product was produced which was analysed by torque evolution. Alteration in PP structure also effected the crystallinity and melting temperature that was studied by thermal analysis. However, percentage crystallinity was enhanced by grafting due to the increase of chain's packing and reduced chain entanglements. MAH-g-PP was used as compatibilizer in 60% PET blends. In all blends, PET's percentage crystallinity was reduced compare to pure PET due to the hindrances of chains packing. Thermal properties of blends were improved as the first melting temperature was observed at 170°C and complete melting of blend occurred on 260 °C. Compatibilizer in PET/PP blend enhanced interactions in the blend resulted in homogeneous blend with less voids. 1% MAH-g-PP was the optimum value of compatibilizer in PET/PP blend that showed maximum uniformity in blend microstructure. Decrease in free space inside the blend hindered water molecules passage through films. Owing to this, water vapour permeability of blend was less compare to pure PET. Nonpolar nature of PP also influenced the water transmittance through the blended films. Blending of PET with PP in the presence of MAH-g-PP improved the processing of PET for film forming. All these properties of this blend make it suitable for packaging application.

Graphical Abstract



Chapter-1

Introduction

1.1: Polymer Blends

Polymer blends can be defined as mixtures of at least two types of polymers, with physical interactions having no covalent bonds between them [1]. Polymer blends can be miscible or immiscible. In miscible polymer blend homogeneous mixture occur and for which ΔG and ΔH are negative. Immiscible blends of polymer mixture is nonhomogeneous due to less compatibility with ΔG and $\Delta H > 0$. To convert immiscible polymer blend to miscible blend, compatibility between polymers is enhanced by modifying the interphase that will reduce the interfacial energy [2].

A group of researchers assume that miscibility of polymer blend can be observed by studying glass transition temperature (T_g). Any blend having two or more T_g is immiscible. But later it was proved to be vary from case to case. There were rare examples seen in which totally immiscible blends showed a single step of T_g and completely miscible blend displayed two steps in differential scanning calorimeter (DSC). T_g of polymer blend depends on the weight, blend's composition and also on the conditions of mixing [3, 4].

Phase separation was also observed in homogeneous blends by varying temperature up or down in phase diagrams of polymer blend two types of critical temperature exist shown in figure 1.1. One is upper critical solution temperature UCST and other is lower critical solution temperature LCST. Blends that are endothermic exhibit UCST. In this case below the critical temperature mixture exist in two phase system and with increasing temperature from a fixed point complete miscible one phase blend can form.

For exothermic systems generally LCST behaviour occur in which one phase can be achieved below a critical temperature. Polymer blends most commonly show LCST behaviour. To obtain a homogeneous phase, free energy of mixing should be negative.

$$\Delta G_{mix} = \Delta H_{mix} - T\Delta S_{mix} \dots\dots\dots 1)$$

Flory Huggins developed a simple model to calculate free energy of mixing of polymer blend and interaction parameter between two polymers.

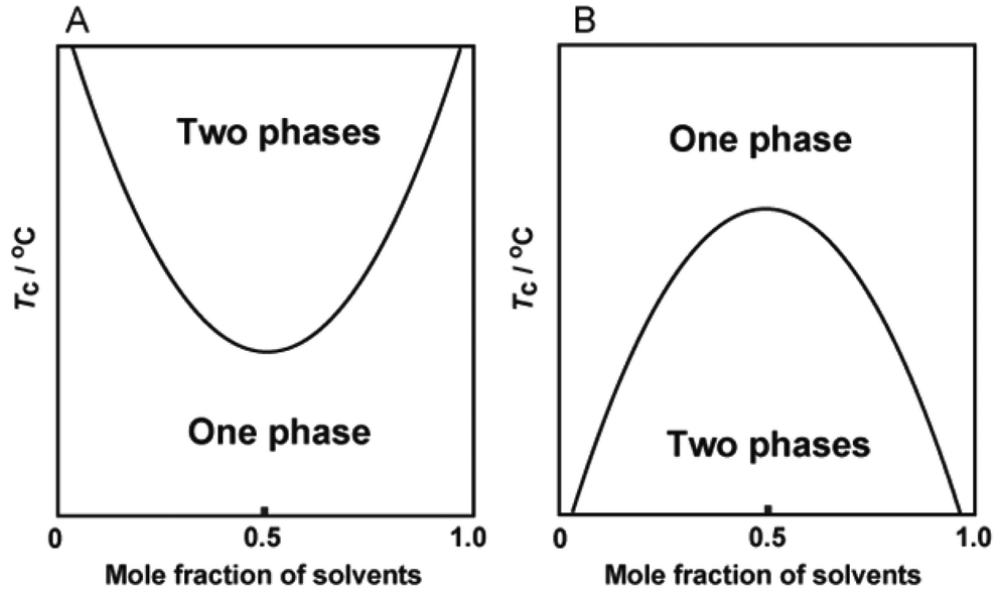


Figure 1.1: Phase diagrams showing A) LCST and B) UCST for polymer blends [5].

$$\Delta G_{mix}/RT = (\phi_1/V_1) \ln \phi_1 + (\phi_2/V_2) \ln \phi_2 + (\chi_{12}/V_1)\phi_1\phi_2 \dots\dots\dots 2)$$

χ_{12} = Interaction parameter between two polymers

ϕ_i = Volume fraction

V_i = molar volume

Miscibility of polymer blend significantly depends on $(\chi_{12}/V_1)\phi_1\phi_2$ term [6-9].

About 60-70% polymer blends comprises of polyolefin. Polyolefin blends are generally economical for developing a material with desirable properties for a particular application.

Blending of polyolefin with engineering polymers can enhance its properties and lower its cost. The barrier and mechanical properties of a blend depend upon its phase separation. Usually hetero phased system doesn't give superior barrier and improved toughness of polymers. The miscible portion of a blend can reduce the solubility of permeate hence

Part of this chapter was submitted as review article for publication.

reduces permeability. Miscibility can be achieved by creating linkages such as, short time cross linking or reversible crosslinking, by introducing ionic interactions or hydrogen bonding. However the most common method is inclusion or generation of medium that will improve the interfacial properties in polymer blends, which has been one objective of this research work.

Mostly the characteristics of blends remains in between of its components when tested individually but preferably due to high compatibility their combined effects increases. Blends of different polymers are made to improve its properties required to become suitable for packaging and maintaining its original properties. Different types of physical and chemical interaction during blending can be cooperative to extend tortuosity and to suppress the permeation of gases [10].

1.2: Reactive Extrusion

The development of new polymers has been reduced considerably and instead of this, modifications in the existing polymers by reactive blending is the latest research. In reactive extrusion process, formation and modification of existing polymers have been done simultaneously with its processing and molding. In reactive extrusion, process is done at less residence time so the chances of degradation of product is low. Following are the types of reaction that can be done in reactive extrusion.

- Free radical, cationic, anionic, coordination and condensation polymerization of monomers. Crosslinking and controlled degradation of existing polymers (e.g. polyolefin) by using initiator that can form free radical for the objective of developing a product with controlled molecular weight distribution and a higher amount of reactive positions for the grafting of any other functional group.
- Functionalization of commodity polymers for the need of forming materials that are required in different applications.
- Polymer's modification by grafting of one type of monomers or mixture of monomers onto the main chain of existing polymers for the objective of enhancing characteristics of the initial material.

- Interchain copolymer production. Usually, this type of reaction can be done by a combination of reactive groups from several types of polymers to form a graft copolymer.
- Coupling reactions which can be done by the reaction of a homopolymer with a polyfunctional coupling agent or a condensing agent to build molecular weight by branching or chain extension.

Two types of screws can be used in twin screw extruder: corotating and counter rotating twin screw extruder. The corotating twin screw extruder works by transferring material from one screw to other, by this good mixing of melt can be achieved. High shear rate is achieved by this with reduced feeding behavior. In counter rotating twin screw extruder, the crest of one screw wipes the flight and clearance of other screw. These types of screws has low clearance that's why it has good feeding behavior.

The viscosity of any reactive system is the most vital property and its knowledge is important in the design of the equipment used in processing. Although, there is no model developed to explain the viscosity of any reactive system which span a broad range of values from polymer solutions to polymer melts, it may be related as a function of several variables:

$$\eta = \eta (\gamma, T, P, M, \xi)$$

where γ denotes the shear rate, P represents pressure, T denotes temperature, M represents molecular weight, and ξ is a measure of the extent of the reaction.

Initiator selection is important for grafting reaction and should meet following criteria: less toxicity, appropriate half-life, adequate hydrogen abstraction capacity, low volatility and high initiator efficiency. Increasing the amount of peroxide will reduce the half-life of initiator [11, 12].

1.3: Plastics based Food Packaging

Food Packaging is used to protect food, to enhance its shelf life and to transport it safely. Packaging include a systematized system of preparing goods for storage, transport, retailing, distribution and end use. A mean of making certain safe delivery to the final

consumer in sound condition at optimum price and a techno-commercial purpose aimed at optimizing the market costs of transport while maximizing sales and eventually profits [13]. Packaging has also been explained as a 'complex structure, technical, dynamic, artistic and contentious segment of business'. Packaging is definitely dynamic and is constantly improving. New materials need new techniques, new techniques require new machinery, new machinery results in upgraded quality, and upgraded quality initiates new markets which require modification in packaging [14].

Packaging performs a series of disparate tasks. The primary functions of packaging have been identified:

Containment: It is dependent on the product's physical appearance and nature. Without containment, product loses its flavour. The containment role of packaging makes a large benefaction in protecting the environment from innumerable of products that are passed from one place to another destination on various occasions every day in any modern society.

Protection: Protection from mechanical destruction during handling. This is often considered as the primary function of the package: to prevent its contents from environmental factors such as water vapour, small molecules gases, microorganisms, odours, shocks, dust, vibrations and compressive forces. The packaging should protect the food product from both mechanical damage during transportation and damage by the climate(s) through which the package will move during distribution and storage in the home.

Convenience: Packaging's important function is in meeting the demands of consumers for convenience. Convenient packages promote sales. For a product that is not entirely consumed when the package is first opened, the package should be reseal able and retain the quality of the product until completely used. Effortless opening must be tempered by seal integrity. The container for shipping as well as the primary packaging must provide comfort at all stages from the packaging line, through storehouse to distribution, as well as completing the needs of the user of the food product.

Communication: There is an old saying that "a package must protect what it sells and sell what it protects." The new techniques of consumer marketing would loss if will not

work for the messages communicated to user by the package. The ability of user to immediately recognize products through distinctive shapes, branding and attaching label enables supermarkets to work on a self-service basis. Not only should the product be identified and the legal requirements of labelling be fulfilled, but often the packaging is an important feature in enhancing sales [13-15].

Above mentioned four functions of food packaging are interconnected and all must be estimated and remembered simultaneously in the package development process. The food packaging has to face different types of environment during the performance. It will be physical environment which can cause a physical damage like damage during transportation due to vibrations, impact by sudden drop, compression during stacking will squeeze or press the product and disfigure it. Product may also impair due to ambient environment in the surrounding of package particularly water vapours, O_2 molecules, heat, light commonly UV radiations. Package also has to interact with human environment to aware them about the product specifications, nutrients and net weight [13].

The quality of the packed food is directly related to the packaging material uses. Most food products damages in quality due to diffusion phenomena, such as moisture absorption, oxygen invasion, flavour loss, undesirable odor absorption, and the migration of packaging components into the food. These phenomena can occur between the food product and the atmospheric environment, between the food and the materials used for packaging, or among the heterogeneous contents in the food product. Hence, mass transfer studies on the transfer of package ingredients and food contents, on the absorption and desorption of volatile material, flavours and moisture, on gas permeation, and on the reaction kinetics of oxidation and ingredient degradation are necessary for system designs of food packaging [16, 17].

The establishment of new packaging functions may go hand in hand with the development of new processes, materials and equipment. The major function of food packaging is barrier protection against the attack of micro-organisms and has a huge impact on product quality. Number of materials are available today, in which the manufacturers have prepared a combination of layers of different materials to give a perfect

package with the barrier properties demanded. These layers can include foil, different types of plastic, paper, and adhesives [18].

Wood, paper folding Cartons, metal such as steel and aluminium and glass were at first used for packaging purpose with extension of packaging application, plastic material showed remarkable development in food packaging. The explanation of this growth in packaging industry are

- 1) Plastic materials offers good mechanical and barrier properties.
- 2) These materials are lighter than metals, wood and glass.
- 3) Plastics offers range of design capacities and features that are not available in any materials.
- 4) Plastics are easily mouldable, can flow and can be made in the form of sheet and films.
- 5) Most of the plastics are cost effective.
- 6) Provide range in colour, transparency and heat resistance.

Properties of plastic materials can be set according to the requirements. Plastic materials shows considerable resistance to inorganic chemicals including organic solvents, acids and alkalis so these can be used for food packaging as these materials do not favour the growth of microorganisms. Thermoplastic polymers can be easily shaped, moulded and recycled although separation poses few limitations [19].

1.4: Polymers Permeability

Principle

Polymer permeability is the defined as the transport of molecules through a film of finite thickness. In the lack of microvoids, passage of gas molecules through a polymer based film, is considered to be restricted by the sorption of gases into the matrix of the film. Permeation through film is commonly occur in 3 different stages that are shown in figure 1.2, first the film absorb the penetrant, then process of diffusion occur through the matrix and at last desorption of penetrate at the other side of film. The sorption and desorption of gas molecules is a rapid action in contrast to the rate of diffusion through the polymer film [20].

Theories of Polymer Films Permeability

Thomas Graham was the scientist who first conducted research study on the permeation of gas through polymer in 1866.

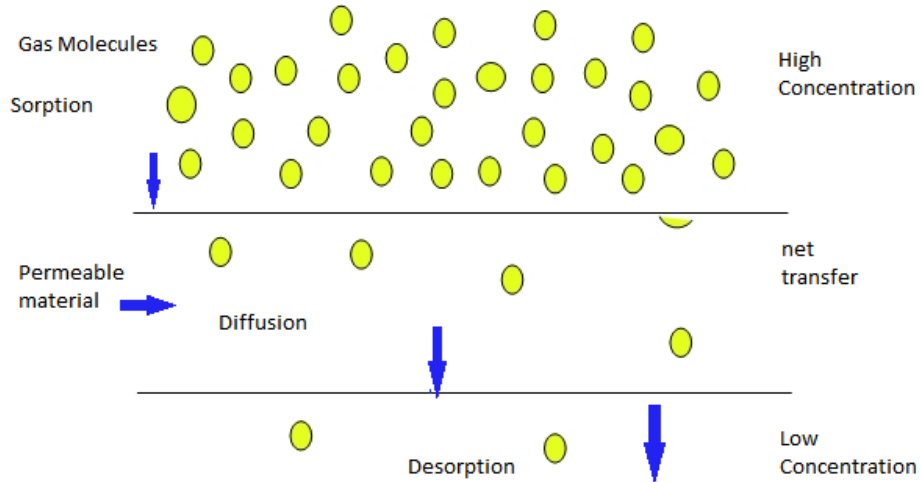


Figure 1.2: Permeation of a substance through a plastic packaging material [21].

He assumes some process during his observation that increasing temperature will increase the permeability and it is independent of pressure. He postulated that variation in film thickness affect the permeation rate but not the separation characteristics of the polymer [22].

In 1855 law of mass diffusion of Fick described as

$$J = \frac{D\Delta c}{l} \text{-----3)}$$

where J is diffusion flux ($\text{mol cm}^{-2} \text{s}^{-1}$) Δc is the difference in concentration (mol cm^{-3}) across the film with thickness l (cm) and D is diffusion coefficient.

Dissolution and diffusion of penetrating substance through the film has great impact on the permeability. At the steady state of diffusion process Henry’s law of solubility states that

$$P = D.S \text{-----4)}$$

“Permeability is the product of solubility coefficient and diffusion coefficient.”

As,

$$S = S_0 e^{-\Delta H/RT} \text{-----5)}$$

And,

$$D = D_0 e^{-E_D/RT} \text{-----6)}$$

$$P = (D_0 e^{-E_D/RT})(S_0 e^{-\Delta H/RT}) \text{-----7)}$$

$$P = P_0 e^{-E_P/RT} \text{-----8)}$$

where P_0 , D_0 and S_0 are pre exponential factors, E_D and E_P are excitation energies for diffusion and permeation respectively.

$$E_P = E_D + \Delta H \text{-----9)}$$

ΔH is the heat of sorption, R is general gas constant and T is temperature (K).

The activation energies for the process of permeation is small in the case of oxygen, and mostly depends on the properties of the gas-polymer interaction. However, it has been shown that D_0 , P_0 and S_0 in eq. 5,6, 7 are related to the size and density of the free volume within the polymer film matrix at the standard temperature [23].

Permeability coefficient depends on various parameters that are properties of the penetrating molecules and film, their interaction and the concentration of penetrating molecules across the packaging film. Permeability coefficient is defined as “ The rate at which a specific quantity of permeating molecules passes through a unit surface area of film in unit time having unit thickness with a unit pressure difference (ΔP) under steady state condition”[21, 22, 24].

Permeation Units

A number of techniques have been designed to measure the permeation of water vapours and gas molecules through polymer films therefore many units are conveniently interconvertible. Unit of permeability can be deduced from eq.

$$P = q \times t / A \times \Delta p$$

where q is the mass flux of gas molecules through a film of thickness t and area A , under a partial pressure gradient Δp across the film. According to researchers working on the

permeability of polymer films expressed q in $cm^3(\text{STP}).\text{sec}^{-1}$, A in cm^2 , t in cm or m , and Δp in $cm\text{ Hg}$ or atm .

Table 1.1: Values of water permeability and oxygen permeability of various commercial plastic used in Packaging [25].

Material	Oxygen Permeability $cm^3\text{ mm m}^{-2}\text{ d}^{-1}\text{ bar}^{-1}$ at 23 °C	Water Vapour Permeability $g\text{ mm m}^{-2}\text{ d}^{-1}\text{ bar}^{-1}$ at 25 °C	Solvent Chemical Resistance	Cost per kg € [26]
HDPE (film extrusion)	40	0.25	good except nonpolar	1.39
PP (co polymer)	60.5	0.55	good except nonpolar	1.27
LDPE (film grade)	190	0.69	good except nonpolar	1.40
LLDPE (film grade)	190	0.6	good except nonpolar	1.33
PET	1.7 (amorphous) 1.4 (semicrystalline)	1.8	good	1.43
PA6	0.98-1.02 (50% RH)	2.33-2.63	excellent	2.48
SAN	0.40	2.0	fair	2.13
ABS	40	5.0	poor	2.05
PS	160	2.0	poor	1.74

Alter suggested that the permeability coefficient can be described in terms of the unit called as “Barrer”[27].

$$10^{-10} \frac{cm^3(STP) \times cm}{sec \times cm^2 \times cm Hg}$$

Permeation properties of packaging films can be a source to estimate the quality of food product. For the purpose to enhance the shelf life of food, barrier properties against low molecular weight gases and water vapours should be high.

Due to the improper barrier properties of packaging films, Food may lose its flavour, colour and nutrients. Owing to this need, blending of polymer, utilizing novel processing technologies that provide efficient films with multi-layered structures, nanocomposites and coatings on plastic films have been developed that upgrade the food packaging films.

1.4: Research Objectives

The aim of this research was to design and fabricate an easily processable packaging material which would have ideal thermal and water vapour barrier properties. Polyolefin (PE, PP) has strength, flexibility, stability, lightness, low cost, ease in process ability, high chemicals and moisture resistance. Polypropylene (PP) is stiffer, denser and more transparent than Polyethylene (PE). It has extremely effective barrier properties for water vapour. PP has low thermal resistance and is not favourable while using microwave. Polyethylene terephthalate (PET) has superior gas barrier, glass like clarity, and light weight. PET has notable aroma barrier owing to this food packed in PET film will sustain its flavour and smell. However PET is not good in moisture repellence compared to Polyolefin and has some process restriction for film molding due to its high T_m .

A homogeneous blend of commodity polymer that will have high water barrier with an engineering polymer having high thermal properties was suggested for economic and recyclability aim, instead laminated, metalized or coextruded structure. PP and PET are approved for food contact during storage. PET resist corrosion and also microorganisms. The miscibility of the components depends on several factors involve interfacial tension, adhesion between two phases and melt viscosities of the components. The change in free

energy of the mixture ≤ 0 is an important condition for miscibility. The change in Gibbs free energy of the mixture is equal to

$$\Delta G = \Delta H - T\Delta S$$

This blend should achieve the lowest possible free energy to become a stabilized homogeneous mixture.

PP and PET can only be miscible if both have same chemical nature. If one component is polar the second component should also be polar to generate attraction. In this case PP is nonpolar and PET has polarity owing to this their blend in any composition can never be one phase. There is need to generate some polar group on PP to generate its compatibility with PET. PP can be functionalized by grafting a polar group on its main chains that will later develop linkage to PET chains.

A homogeneous blend can provide optimum barrier, mechanical, thermal and optical properties. A blend formation is cost effective as compare to the development of a new homopolymer having all superior properties or the addition of additives and fillers in polymer matrix. Polymers used in food packaging are mainly categorized into two major group according to price. Polyolefin, PS and PVC are considered to be low cost, recyclable and simpler thermoplastic materials. On the other hand, PET, Polyamide, EVOH, PLA and biopolymers are expensive and difficult to process. PP with good water vapour resistance is easy to process than HDPE therefore preferable. PET with high oxygen barrier properties has high transparency and good strength. A homogeneous blend of these two polymers will ultimately provide a combination of required properties.

The main objectives of this research work are listed below:

- 1) Principal objective is to develop reactive extrusion process of grafting of maleic anhydride (MAH) on the main chain of Polypropylene to obtain MAH-g-PP.
- 2) Secondary objective is to explore and demonstrate application of the developed compatibilizer such as to develop homogeneous blends of PP and PET and to develop plastic films based on blend and measure its water vapor transmission rate.

Chapter-2

Literature Survey

2.1: Barrier Properties of Polymer Films and Functionalized Food Packaging Films

Dispersion of materials in nanometre range in polymer films during the past few years showed remarkable improvement in the barrier properties as well as acted as reinforcing materials to raise mechanical strength. Nano materials with particle size less than 100 nm in one dimension provides effective interaction with polymer chains reducing voids and pores results in resisting small molecules and water vapour to pass through the films. Surface area and surface energy of particles play a significant role in the enhancement efficiency. Due to this strong interaction of nano sized materials with polymer chains, approach of these additives or fillers to the food inside the film, diminishes. Owing to that food products' flavour and colour will maintain. During the past decade, nano structures of different geometry and dimensions are being utilizing in research on food packaging films as well as in food packaging industries to improve the barrier properties of films. Weight percentage of nano sized filler also have great impact on the end product's properties. There is a need to disperse nano particles uniformly throughout the matrix to increase interfacial area of matrix and filler. This will restrict the movement of matrix and improve its barrier properties. Commonly used nano sized materials in food packaging films are nano clays, metal oxides and carbon based nano structures [28].

Most of the researchers studied Montmorillonite (MMT) clay, a natural clay used in food packaging application, structure of MMT clay is displayed in figure 2.1[29]. In MMT clay, a central octahedral sheet is sandwiched between two tetrahedral sheets as shown in figure 2.1. In tetrahedral sheets, oxygen atoms are involved to silica linking tetrahedral sheets and form hexagonal network. In octahedral sheet, aluminium or magnesium is linked with oxygen forming octahedral sheets [30, 31].

Exfoliation of clay forming nano layers in polystyrene was investigated in 1999. Functionalization of MMT clay by vinylbenzyltrimethylammonium chloride

(VDAC) was done to form highly exfoliated clay polystyrene nano composite. Functionalized Ca^{+2} MMT and Na^{+} MMT in PS nano composite was synthesized and highly exfoliated structure was detected. A higher thermal degradation temperature than pure PS was observed [32].

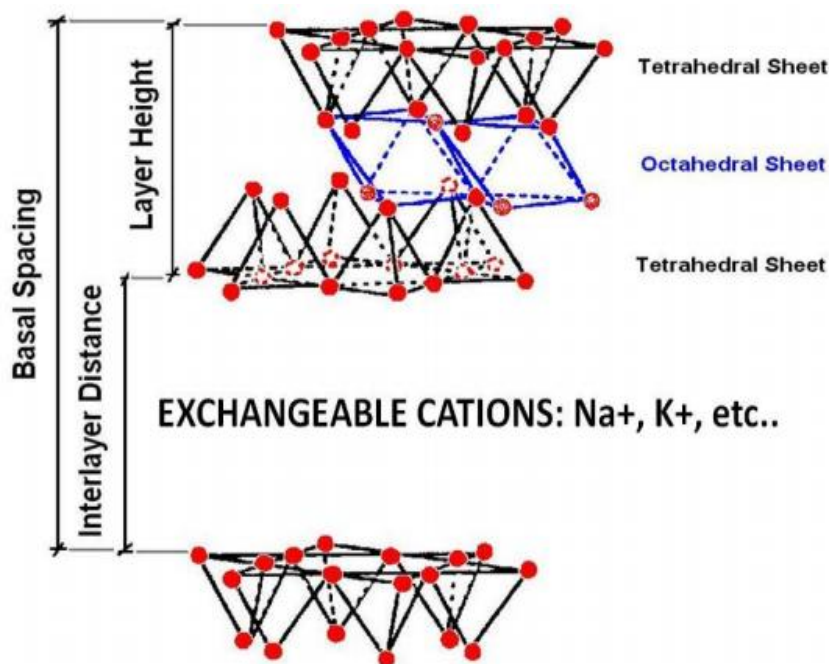


Figure 2.1: Structure of Montmorillonite Clay [33].

After surface treatment of MMT clay with octadecylamine, added in polyester amide. Mechanical and barrier properties of extruded and compression moulded films were studied like the above work, an increase in mechanical properties was observed but there was no much influence on the barrier properties due to voids present in the film. X ray diffraction data showed that sheets of clay particles were not uniformly dispersed throughout the matrix [26].

In another research, dynamic melt mixing process was used for the delamination of clays in EVOH matrix. MMT clay was treated same like the prior mentioned work and mixed morphology was obtained influencing its permeability. On the other hand this compatibilizer prominently decreased the T_m , T_c and also degree of crystallinity of composite as compare to pure EVOH [34].

Furthermore, contribution of geometric factors on the barrier properties of PCNs was investigated and it was observed that the aspect ratio of silicate platelets is a crucial factor that controlled the permeation of gas and vapours through films. Barrier properties can be control by aspect ratio and clay content [35].

Not only was the aspect ratio, other characteristics of clays and effect of these parameters on the permeability of films analysed in another study on PCNs. It was predicted that increase in clay layer spacing and chain confinement results decrease in permeability [36].

Clay's dispersion in polymer matrix, polymer blends and or utilizing various processing techniques to exfoliate the clays layers proffer packaging films with high tortuosity. This propitious tortuosity will enlarge the diffusive path of O₂, CO₂ and water vapours providing high barrier films used in packaging applications. This mechanism is explained in figure 2.2.

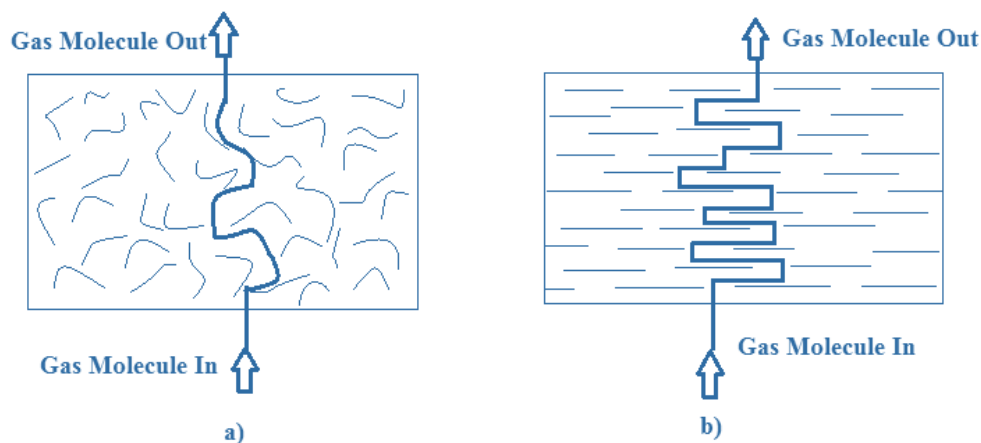


Figure 2.2: Effect of Clay's dispersion on the tortuosity of films a) random disorient clay in film b) highly oriented well dispersed clays offers high tortuosity.

For the sake of reduction in cost of packaging films, low amount of this nano clay filler will offer less permeability. Owing to high surface area of particles, disperse easily in addition to this interact with more polymer chains. Functional group of our requirement to enhance compatibility can be added on the surface of clay by modification.

Modified clay provides increase in the compatibility with different plastics. The greater the compatibility between clay and polymer matrix, lesser will be the voids that will lower its permeability [37-41].

Apart from clay, several other publications exposed on the improvement of the barrier properties of films using graphene. It was described that the dispersion of graphene sheets in polymer reduces the permeability of the films that can be employed in food packaging [42]. Dispersion can be improved by various chemical modifications. Graphene sheets originated from the exfoliation of graphene oxide after chemical modification can be dispersed well in polymer matrix after applying surfactants to inhibit restacking of sheets. Permeability of oxygen and other gas molecules falls significantly using graphene sheets as compare to organically modified MMT clay and other filler having nano sized dimensions [43, 44].

There are several techniques employed to complement to enhance the barrier properties of plastic packaging film. For example coating of thin metal film of few micron is done to incorporate metal like barrier properties. Physical vapour deposition (PVD) is the most important technique used commercially in the coatings of thin films on polymer surface. A common metal coat by this process is aluminium. Thickness of thin film can be controlled by vaporization and adhesion of metals on surface. There is a limitation in this process that PVD will provide coatings with pin holes and defects that will allow some of the molecules to pass and ultimately barrier properties will not be much effective. This can be overcome however with modern coating process that provide uniform coating. PP, PET, PS and PVC films usually metalized by this technique [45].

Transparent coatings of Al_2O_3 and SiO_2 by vacuum deposition method coated on polymer films used for food packaging allows the product to be visible with high level of barrier that is required and also cost effective. Alumina when coated by thermal evaporation on bi oriented PP (BOPP) and PET, showed surface defects that depends upon the coatings nucleation, growth and also structure. These imperfections in the coatings as a result allow the passage of oxygen molecules and water vapours. It is deduced that if defects free coatings are formulated by changing process parameters resistance can be enhanced for the diffusion of small gas molecules. Role of the nano defects and micro

defects on gas permeation of barrier films was also explained for SiO₂ coatings on PET. Three types of defects are usually present in barrier films; micro defects that allow the pass of molecules and size of these imperfections are 3 or 4 times of permeate molecules, next is nano defects that somehow resist the transmission and last is permeation through amorphous lattice. Overall improvement in the barrier properties of the films was suggested to be clearly dependent on the population of defects in the coatings [46, 47]. Figure 2.3 explains the passage of gas molecules through these upper mentioned three types of imperfection. Defects in coatings formed by PVD can be controlled by deposition technique, deposition time, deposition temperature and pressure, deposition position in the chamber and wafers' orientation and rotation modes [48].

To achieve defect free coatings on polymer films surface another beneficial technique "Atomic Layered Deposition" utilized to reduce the permeability of the film. By this approach layer can be easily controlled as one deposition cycle deposit only monolayer. This process can easily substitute aluminium foil in food packaging due to its advancements in the barrier properties. BOPP, Polylactic acid (PLA) and PET when nano coated with alumina by using atomic layer deposition it gives remarkable magnification in barrier. Furthermore, it was deduced that plasma pre-treatments can additionally reduce the permeability of packaging films [49].

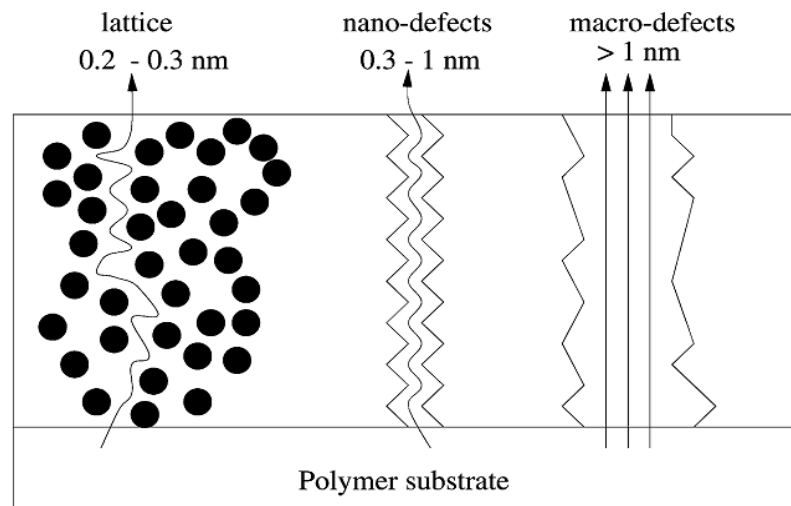


Figure 2.3: Transmission of gas molecules through oxide coatings[47].

By controlling temperature during plasma assisted Atomic layer deposition (ALD), barrier properties of alumina on polymer films can further be enhanced. It was reported that low deposition temperature for alumina is suitable that resist 20nm alumina nano coating on PEN by PA-ALD, it was stated to hinder moisture and oxygen molecules perfectly. Another factor that play vital role is thickness of nano coatings and polymer film [50].

Effect of thickness of alumina coating grown through ALD technique at low temperature was investigated and it was concluded by experiment that thinnest nano coating of polymer films mostly provides enhanced coverage and decrease the transmission usually 25-100nm thin layer is enough to resist oxygen molecules and water vapours. Greater the thickness of film higher the chances of cracks growth in coatings and defects will start to generate that will ultimately allow the moisture and small molecules to permeate through the film [51].

CVD grown film on polymer substrate is also another process which is studied by a research group. Plasma enhanced CVD nano coatings with ALD technique was experimented. Alumina by ALD with 5nm thickness and SiN by PE-CVD with 10nm thickness multi-layered coating on polymer substrate was reported to be ultra-barrier packaging film. It was supposed that low density columnar boundaries in SiN reduce WVTR [52].

2.2: Polymer Blends in Food Packaging

Among the most widely employed blends generated with improved properties are PP/PET, PP/Nylon[53], PLA/PBS[54], EVOH/PP[55], EVOH/PE [56] and PP/PLA [57] PE/PET[58]. Polyolefin usually polyethylene (PE) and polypropylene (PP) are in use on a large scale for the packaging of the foodstuff due to its low price and safety in food packaging. But these types of films have no strong barrier against water vapours, CO₂ and O₂. It will allow the passage of small molecules through the film that will eventually spoil the food due to the loss of colour, flavour and nutrients. Most of the market is dominated by polyolefin. Researchers are working to improve barrier of polyolefin by blending with a high barrier polymer e.g. polyamide, EVOH and PET [59]. Most of the Polyolefin blends do not show a remarkable influence on the barrier properties. However, by the addition of

either compatibilizer e.g. by adding some ratio of PP or PE grafted maleic anhydride (PP-g-MA or PE-g-MA) with original PP/PE or by using maleic anhydride grafted PP/PE as whole with high barrier polymer [60, 61]. Blending of these polymers was reported to be done in single or twin screw extruder. Permeability can be further reduced by controlling the morphology and to make it homogeneous and well mixed blend with less voids. This can be done by setting the weight ratio of polymer in the blend. Extrusion temperature, screw rpm, time and pulling ratio have influence on the morphology of blend [55, 62-64]. Apart from this, researchers are working on the blend of biodegradable polymer for packaging. Biodegradable polymer are not mechanically strong enough and have moderate barrier properties. Biodegradable materials are usually costly. So there is a great demand to improve its properties and lower its cost. Polylactic (PLA) is biodegradable polymer used in food packaging industry. Its barrier properties are somehow equal to PET and PS but mechanical strength is low [65].

Blend of PP and PLA was made to form a partially biodegradable films with a combination of properties. Characteristics of the blended film can be controlled by adjusting the content of both polymer according to our requirement. PLA when added in PP increased the permeability of water vapours while O₂ was reported to be reduced. Blend of Poly Butylene Succinate (PBS) and PLA was also predicted to be suitable biodegradable material for food packaging. Blend was prepared through the extruder. Both of these polymers are incompatible [54].

A number of compatibilizers used to enhance the interfacial bonding in PET and PP blend. LLDPE-g-MA PP-g-MA and hydrogenated SBS block copolymer were used as compatibilizers. This research on the comparison of all the compatibilizers in PET/PP blend indicated a high efficiency of SEBS-g-MA and PP-g-MA + EPM (ethylene propylene copolymer) but low performance of LLDPE-g-MA and PP-g-MA. EPM was reported to be a promoter in the effectiveness of PP-g-MA. It decreased the interfacial stresses and hindering of the migration of PP-g-MA into PP [66].

The elastomer based compatibilizer efficiently bear the stresses induced at PET/PP interface. In another work maleic anhydride grafted polyethylene octane elastomer (POE) was used in PET/PP blend with 80/20 composition. The results indicated a fine dispersed

phase morphology by the insertion of POE-g-MA. However the modulus, tensile and flexural strength were lowered owing to the softness induced by elastomeric compatibilizer. T_g of PET was shifted to lower value by the addition of a compatibilizer in PET/PP blend [67].

Apart from maleic anhydride other compounds were also used in the blend of PET and PP as compatibilizer. Silane coupling agent (SCA) was added as compatibilizer in PET/PP blend with 20, 40, 50, 60% PET. SCA marvellously improved the mechanical properties of blends. Morphology of the blends showed a better adhesion when SCA compatibilized blends were compared to non compatibilized PP/PET blend [68]. Acrylic acid functionalized PP was used as compatibilizer in PP/PET blends. Blending was done on laboratory scale batch mixer and co rotating twin screw extruder. Functionalized PP induced a very fine dispersed phase morphology. Mechanical properties were prominently enhanced. All these effects were reported to be due to reduced interfacial tension by adding to PP-g-AA [69].

2.3: Grafting of Polyolefin

Functionalization of polyolefin to insert a polar group for enhancing its compatibility with various engineering polymers has been done by many researchers in previous decade. Mostly polypropylene (PP) and polyethylene (PE) are functionalized by maleic anhydride or acrylic acid. Grafting of maleic anhydride or acrylic group on the chain of PP or PE was done by solution and melt techniques.

PP was grafted with maleic anhydride (MAH) by solid phase graft copolymerization. In this process, reaction was done in a four neck glass with an agitator. Reaction was done at 130°C temperature, 100 rpm under nitrogen. Benzoyl peroxide (BPO) and MAH were added in two parts in total 16 min. Reaction was done in 58 min and extracted with acetone to purify the grafted PP from unreacted monomer [70]. Twin screw extruder was also used for the grafting of maleic anhydride on PP by varying MAH and BPO concentration. This reactive extrusion process was done on 150 rpm, under nitrogen with a temperature profile 180, 200, 200, 210, 210, 210, 200 °C. For purification xylene was used. Carbonyl index (CI) was used to estimate the percentage of grafting. DSC, MFI, SEC and NMR were used for confirmation of grafting [71]. Functionalization of PP with maleic anhydride was done

in a batch mixer in the presence of dicumyl peroxide (DCP). Grafting percentage was calculated by varying amount of DCP and MAH at 180 °C and 60 rpm. The properties of grafted PP were investigated by titration, FT-IR, Contact angle measurement and thermal analysis (DSC). Complete reaction mechanism was explored for the grafting of MAH on PP [72]. Effect of PP grafting by maleic anhydride on rheological properties were studied by using twin screw extruder. It was deduced that molecular weight after grafting will ultimately effect the rheological properties. By varying MAH and peroxide concentration molecular weight can be controlled. Higher MAH will degrade long chain of PP and peroxide concentration will also initiate side reaction that will reduce weight average molecular weight of PP but polydispersity index will remain same (PDI) [73]. Grafting of MAH on LDPE was done by reactive extrusion in twin screw extruder at temperature profile 140 °C, 160 °C, 180 °C and 200 °C and 60 rpm. DCP showed a small effect on the viscosity of grafted LDPE. By increasing the concentration MAH, viscosity of grafted LDPE was reduced [74].

Grafting of acrylic acid on polyethylene film's surface was done by specially designed equipment on which film is mounted. At one side there was grafting solution of acrylic acid and on the other side of film, there was air with oxygen that was supposed to inhibit grafting on the other side of film. Gamma irradiation method was used to graft acrylic acid on PE film with controlled yield. This top layer grafted surface will inhibit diffusion through the film [75]. Preirradiated PP was used to graft acrylic acid on PP chain by reactive extrusion mechanism. This method showed a little degradation in pure PP when concentration of irradiated PP was increased owing to high radicals generation. Final product provided a high impact material that was of potential industrial interest [76].

Chapter-3

Experimental Procedures

3a: Preparation and Characterization of Functionalized Polypropylene

3a.1: Materials and Method

The chemicals and materials were used as received without further purification. Maleic anhydride (MAH) was 99% pure obtained from (Sigma Aldrich) with density 1.314 g/cm³, benzoyl peroxide (BPO) that was used as initiator and isotactic polypropylene (produced by LCY Chemicals CORP) with MFI 3.297 g/10min at 190°C and density 0.908 g/cm³ were industrially donated. Acetone was commercial grade, used as solvent for MAH and BPO. Prior to grafting of PP, differential scanning calorimetry (DSC) of 5-7 mg PP sample was done to check that either polypropylene is isotactic or atactic. Melting Temperature (T_m) was 165°C and glass transition temperature (T_g) was at -20° C so it was deduced that PP used for grafting was isotactic.

3a.1.1: Reactive Extrusion for Grafting MAH on Isotactic Polypropylene

For the functionalization of PP, MAH was grafted on PP chain using BPO as initiator. MAH and BPO were dissolved in acetone and PP pellets were added. After volatilizing the acetone, BPO and MAH adhered onto the pellets homogenously. Functionalization of PP was carried out by reactive extrusion process in HAAKE PolyLab OS internal engineering mixer system displayed in figure 3.1. Internal engineering mixer has two counter rotating triangle shaped rotors having rotational speed ratio 1.25:1 (left to right) shown in figure 3.2. Recipe was prepared in internal mixer software HAAKE Polysoft by adding density and processing conditions of materials. The processing conditions were temperature 160°C, screw speed 60 rpm and reaction time was 10 minutes. Barrel was first preheated at 160°C and material was added in two parts. Thermocouple was mounted on the bottom of the mixer to maintain the melt temperature. The change in torque throughout of the reaction was measured from the transducer that was mounted on the

rotating shaft. Process parameters that remain constant were temperature, screw speed and time, MAH and BPO varied by following table 3.1 and table 3.2.

Table 3.1: Experimental design by varying Maleic anhydride and constant BPO.

Sample Name:	Maleic anhydride	Benzoyl Peroxide
	(MAH)	(BPO)
	phr	phr
PM1	0.05	0.4
PM2	0.10	0.4
PM3	0.15	0.4
PM4	0.20	0.4
PM5	0.25	0.4

Table 3.2: Experimental design by varying Benzoyl Peroxide and constant MAH.

Sample Name:	Maleic anhydride	Benzoyl Peroxide
	(MAH)	(BPO)
	phr	phr
PB1	0.15	0.2
PB2	0.15	0.3
PB3	0.15	0.4
PB4	0.15	0.45
PB5	0.15	0.5



Figure 3.1: HAAKE PolyLab OS internal engineering mixer system.

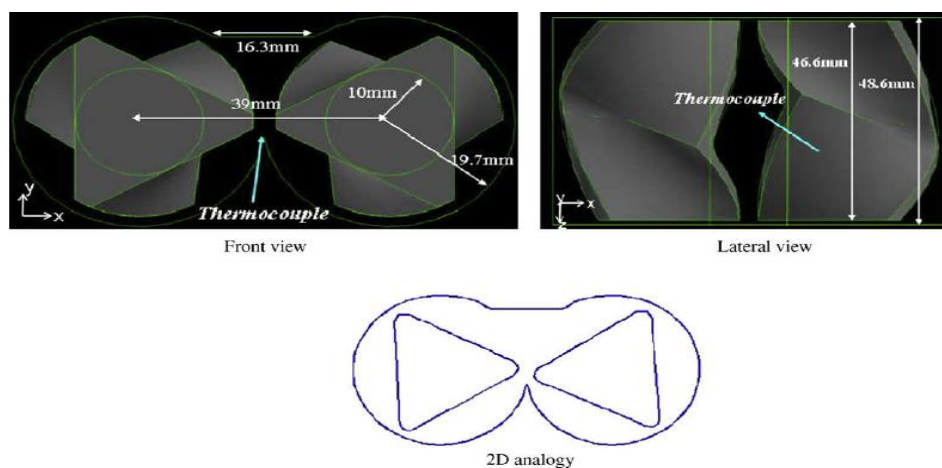
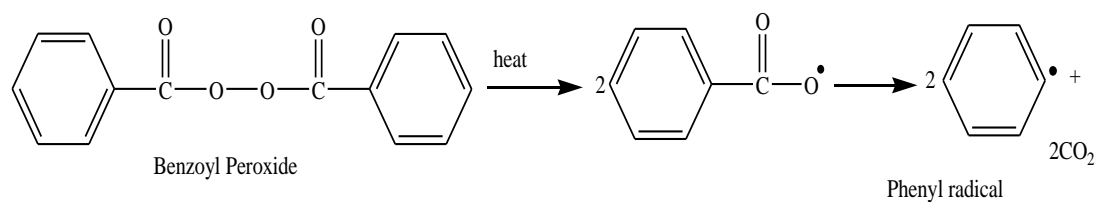
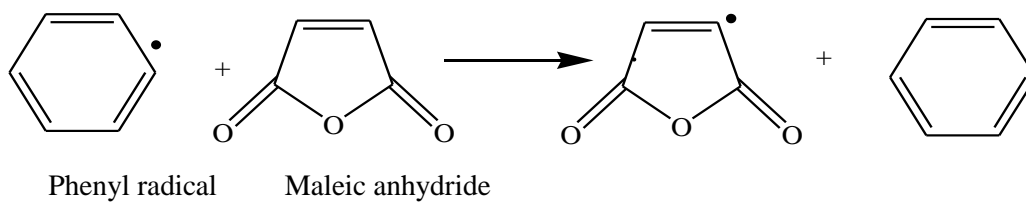
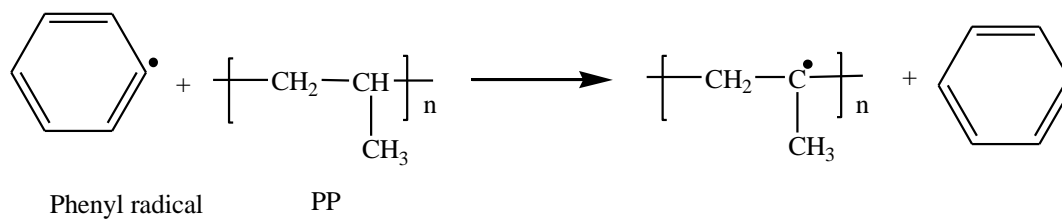
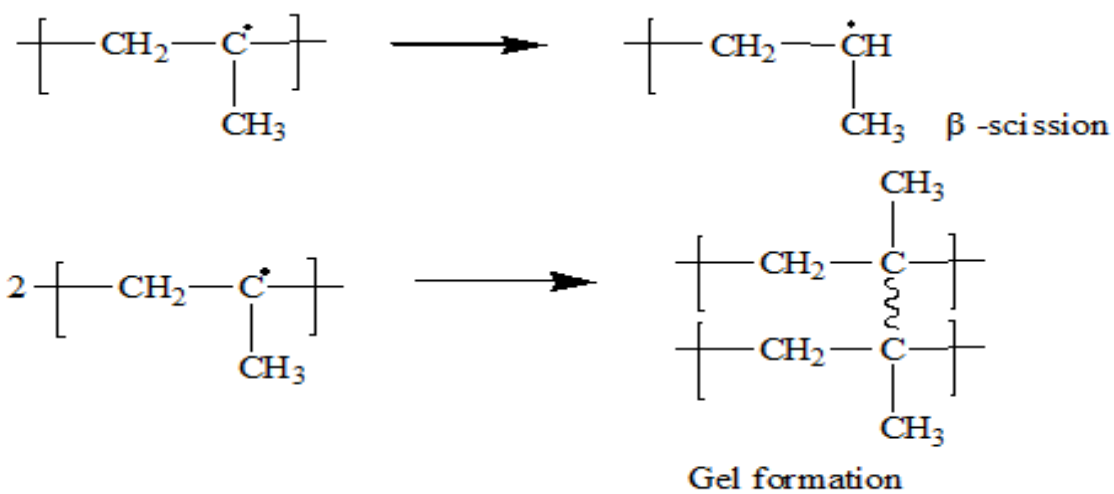
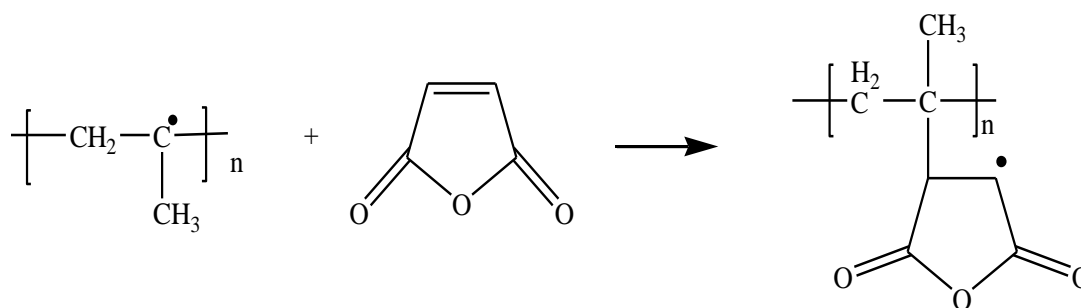


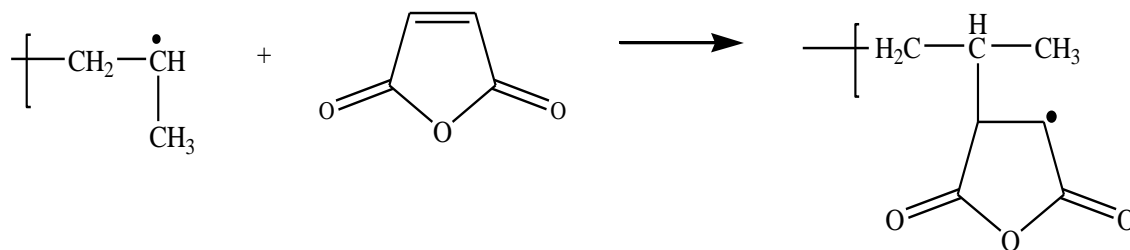
Figure 3.2: Simplified inside 2D view of HAAKE PolyLab OS internal mixer system[77].

A complete reaction mechanism during the grafting of MAH on PP by using BPO as initiator are detailed below.

Decomposition of Benzoyl Peroxide

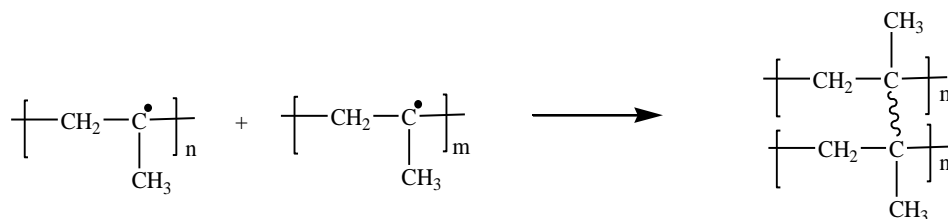
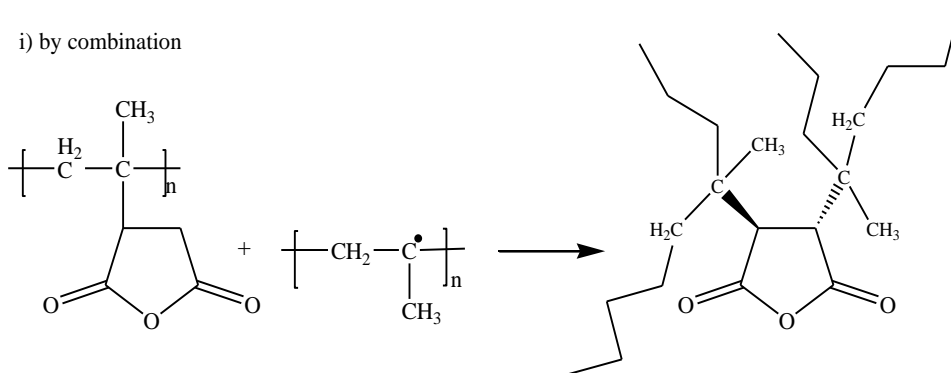


Initiation**Possible side reactions****Grafting of MAH on PP**

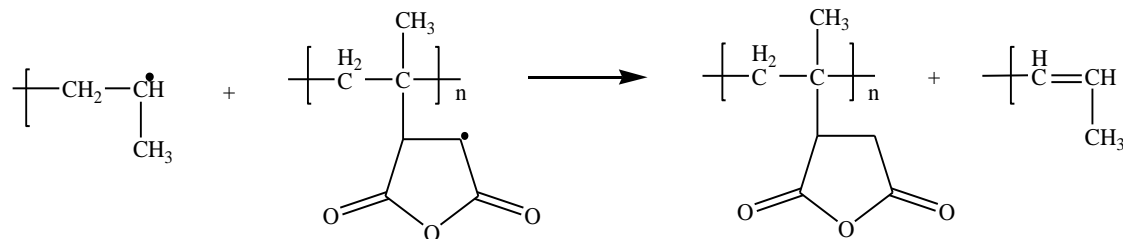
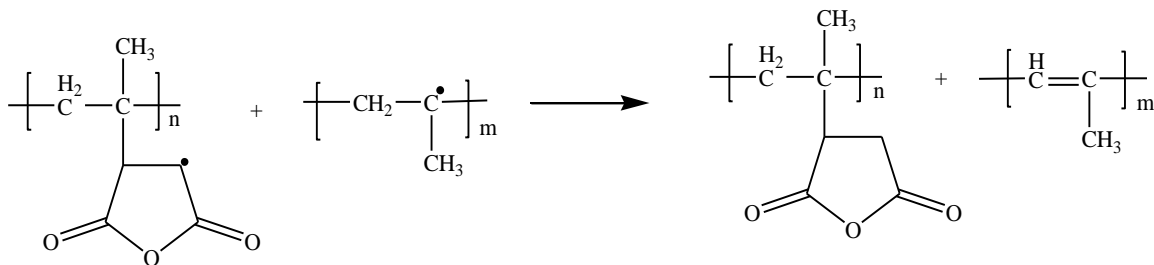


2 Possibilities for Termination

i) by combination



i) by disproportionating



3a.2: Characterization of Grafted PP Samples

During the grafting of maleic anhydride on PP, data obtained from internal mixer was analysed to obtain information about the rheological behaviour of grafted PP. After reactive extrusion process, formulations that obtained were characterized by FTIR, MFI and DSC to confirm this reaction.

3a.2.1: Torque evolution in Internal Mixer

In internal mixer, external sensors are used to maintain a stable environment inside the reaction chamber. Torque was detected by transducer to obtained data about the viscosity of PP during reactive extrusion. This mixer works at defined speed (shear rate) and time, and materials behaviour is recorded as torque. Rotors' rpm is defined, if there is any viscosity change inside material, system will gain more energy to maintain speed of rotors, this will generate signal recorded by transducer. In mixing chamber temperature is controlled by independent heating and cooling zones. When there is friction due to mixing inside the chamber, heat will generate and cause a change in materials temperature. This change in material's temperature is recorded as measuring signal.

3a.2.2: Fourier Transform Infrared Spectroscopy (FTIR)

Fourier Transform Infrared Spectroscopy (FTIR) FT-IR Bruker Alpha spectrometer, spectrum was done to confirm the grafting of maleic anhydride functional group on PP chains. The spectrum was recorded by Bruker Alpha instrument. Spectrum was studied in FT-IR Essentials software. From the FTIR spectra of all grafted samples carbonyl index (CI) was calculated using following equation:

$$CI = A_{1750} / A_{1455} \dots\dots\dots 10)$$

Where, A_{1750} is the area of absorbance peak at 1750 cm^{-1} , that is characteristic of carbonyl functional group from five membered cyclic anhydrides; and A_{1455} is the area of absorbance peak at 1455 cm^{-1} , that is characteristic of the methylene group (CH_2), proportional to the concentration of polypropylene [71].

3a.2.3: Thermal Analysis by Differential Scanning Calorimetry (DSC)

Effect of grafting maleic anhydride on the thermal properties (T_m) of PP was analysed by Differential Scanning Calorimetry. Grafted samples were characterized in a Perkin Elmer differential scanning calorimeter (DSC), by heating 5-8 mg of sample at 10°C/min under nitrogen (N_2) atmosphere from ambient temperature to 200 °C. The values obtained by DSC measurements for the heat of fusion for pure PP and grafted PP samples were utilized to calculate percentage crystallinity by following equation.

$$\% \text{ Crystallinity} = \frac{\Delta H_f^*}{\Delta H_{f100}} \dots\dots\dots 11)$$

where, ΔH_f^* is heat of fusion of grafted PP and ΔH_{f100} is heat of fusion for hypothetically 100% crystalline PP [72]. The value for enthalpy of fusion of 100% crystalline PP used was 207 J/g [78].

3a.2.4: Melt Flow Index (MFI)

To study the effect of grafting on the flow behaviour of PP, MFI of all grafted samples was measured at 190 °C under the weight of 2.16kg in Noselab ATS Plastometer. The analysis was carried out 3 times for each reactive extruded samples.

3b: Fabrication of Polyethylene Terephthalate (PET) and Polypropylene (PP) blends' films

3b.1: Materials and Method

From the samples manufactured in first step, highest grafted isotactic polypropylene was chosen from all grafted samples and was mechanically blended in different proportions with film grade polyethylene terephthalate (provided by Gatron Industries limited) having melting temperature 262.76 °C and glass transition temperature 80.38 °C which was checked by differential scanning calorimetry (DSC) prior to blending, with MFI 39.36 g/10 min at 280 °C under 2.16 kg weight and density is 1.38 g/cm³.

3b.2: Preparation of Blends

Blends of MAH grafted polypropylene and pure polypropylene with polyethylene terephthalate were prepared by varying composition in internal mixer by melt blending. PET was added first then PP and MAH-g-PP were added. Blending was done at 270 °C temperature, 70 rpm and 10 minutes. Samples were cooled on room temperature without any quenching and chains alignment setup. Compositions details are explained in table 3.3.

3b.3: Preparation of Polymer Blends' Film

Blends made in internal mixer were cooled on room temperature. Films of blends were made by injection molding at 200 °C temperature. Films were cooled on room temperature without chains alignment.

3b.4: Characterization of Polymer Blends

Blend of polypropylene and polyethylene terephthalate were characterized by FTIR, DSC, SEM and water vapours' permeability was detected.

Table 3.3: Composition details of PP/ PET blends.

Samples	Film Grade PET (%)	Isotactic PP (%)	MAH-g-PP (%)
Composition 1	60%	39% PP	1%
Composition 2	60%	37.5% PP	2.5%
Composition 3	60%	35% PP	5%
Composition 4	60%	40% PP	-
Composition 5	100 %	-	-
Composition 6	-	100 %	-

3b.4.1: Fourier Transform Infrared Spectroscopy (FTIR)

Fourier Transform Infrared Spectroscopy (FTIR) FT-IR Bruker Alpha spectrometer, spectrum was done to study the specific interactions in the blend of PP with PET by analysing functional groups present in the blend. Generally these interactions can affect stretching frequency of CH₂ from 2950 cm⁻¹ to 2840 cm⁻¹ and also C=O stretching at 1750 cm⁻¹. The spectrum was recorded by Bruker Alpha instrument. Spectrum was studied in FT-IR Essentials software.

3b.4.2: Differential Scanning Calorimetry (DSC)

Thermal analysis of all blends was done by Perkin Elmer differential scanning calorimeter (DSC), by heating 5-8mg of sample from 50 °C to 300 °C at 10 °C per minute scan rate under N₂ atmosphere. There was no effect on the percentage crystallinity of PP in the blend and percentage crystallinity of PET in the blends was calculated by following equation as equation 11.

$$\% \text{ Crystallinity} = \frac{\Delta H_f^*}{\Delta H_{f_{100}}}$$

where, ΔH_f^* is heat of fusion of PET in blend and $\Delta H_{f_{100}}$ is heat of fusion for hypothetically 100% crystalline PET [72]. The value for enthalpy of fusion of 100% crystalline PET used was 140 J/g [78].

3b.4.3: Scanning Electron Microscope (SEM)

Scanning electron microscopy (SEM) Joel JSM 6490A was performed to study the morphology of blends. By analysing SEM images it can be said that whether the blend is homogeneous or phase separated. Fracture behaviour of blends was also investigated by SEM images.

3b.4.4: Films' Water Permeability

Water permeability of prepared films was determined by ASTM E-96. Films were covered on a cup filled with known weight of water and was placed in open air at 29°C and 20% RH. After 24 hrs weight of the water inside the cup was measured and evaporated water was calculated.

$$WVTR = G/tA \dots\dots\dots 12)$$

where

G = change in water weight

t = time during which change occurs

A = test area

From this calculated water vapours transmission rate permeance was measured by equation 13.

$$Permeance = WVTR/\Delta P \dots\dots\dots 13)$$

ΔP = vapour pressure difference

From calculated permeance, permeability of films for water vapours was determined by equation 14.

$$Average Permeability = permeance \times thickness\ of\ film \dots\dots\dots 14)$$

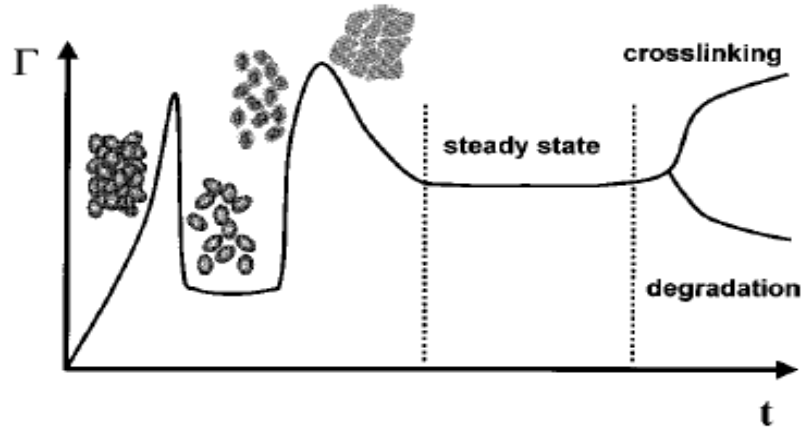


Figure 4.1: Typical torque time curve in internal mixer[79]

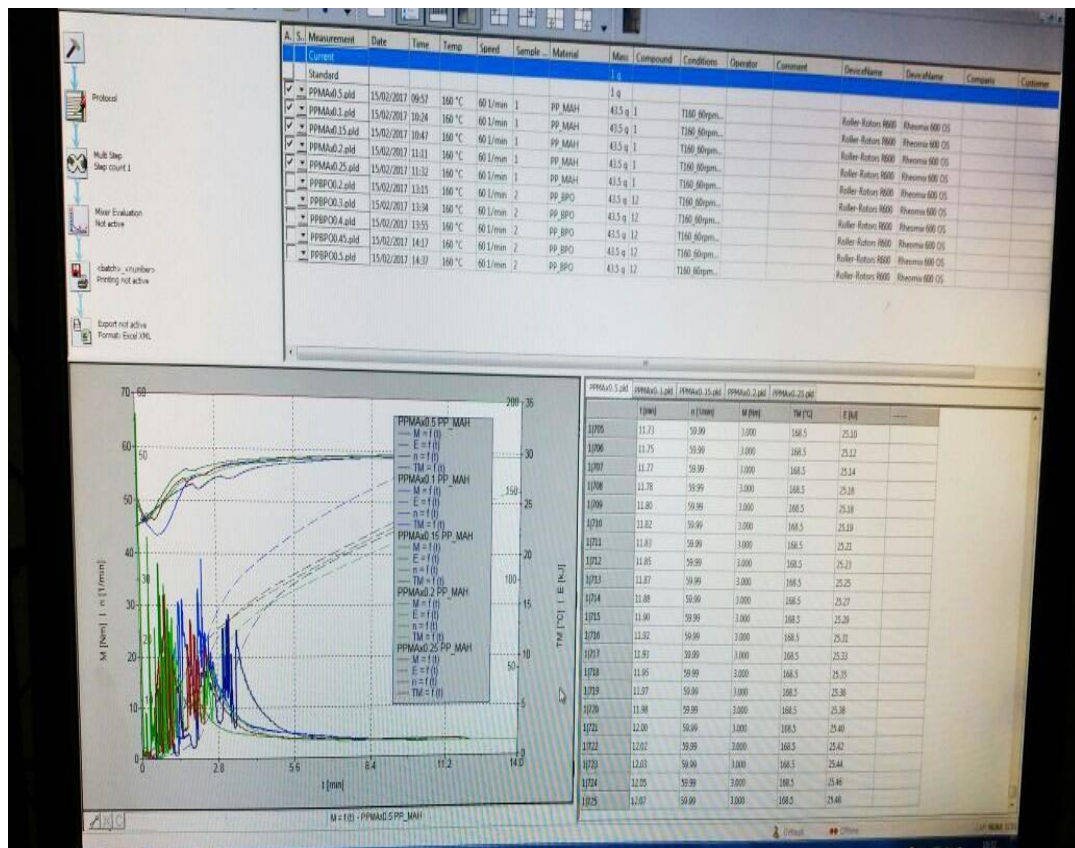


Figure 4.2: Measurement curves generated by HAAKE Polysoft Software for samples having MAH variation at constant BPO.

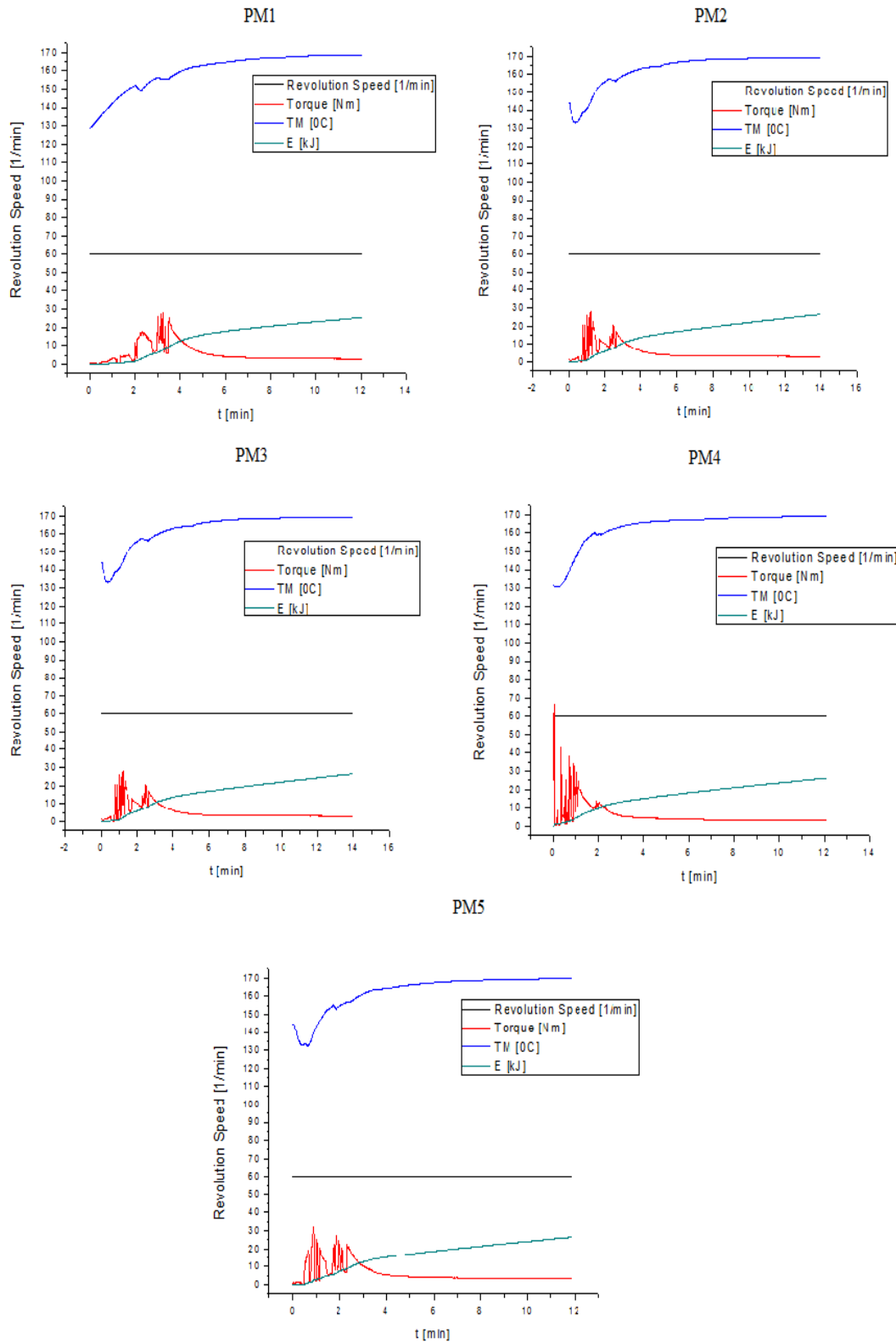


Figure 4.3: Effect on torque by varying MAH content at constant BPO.

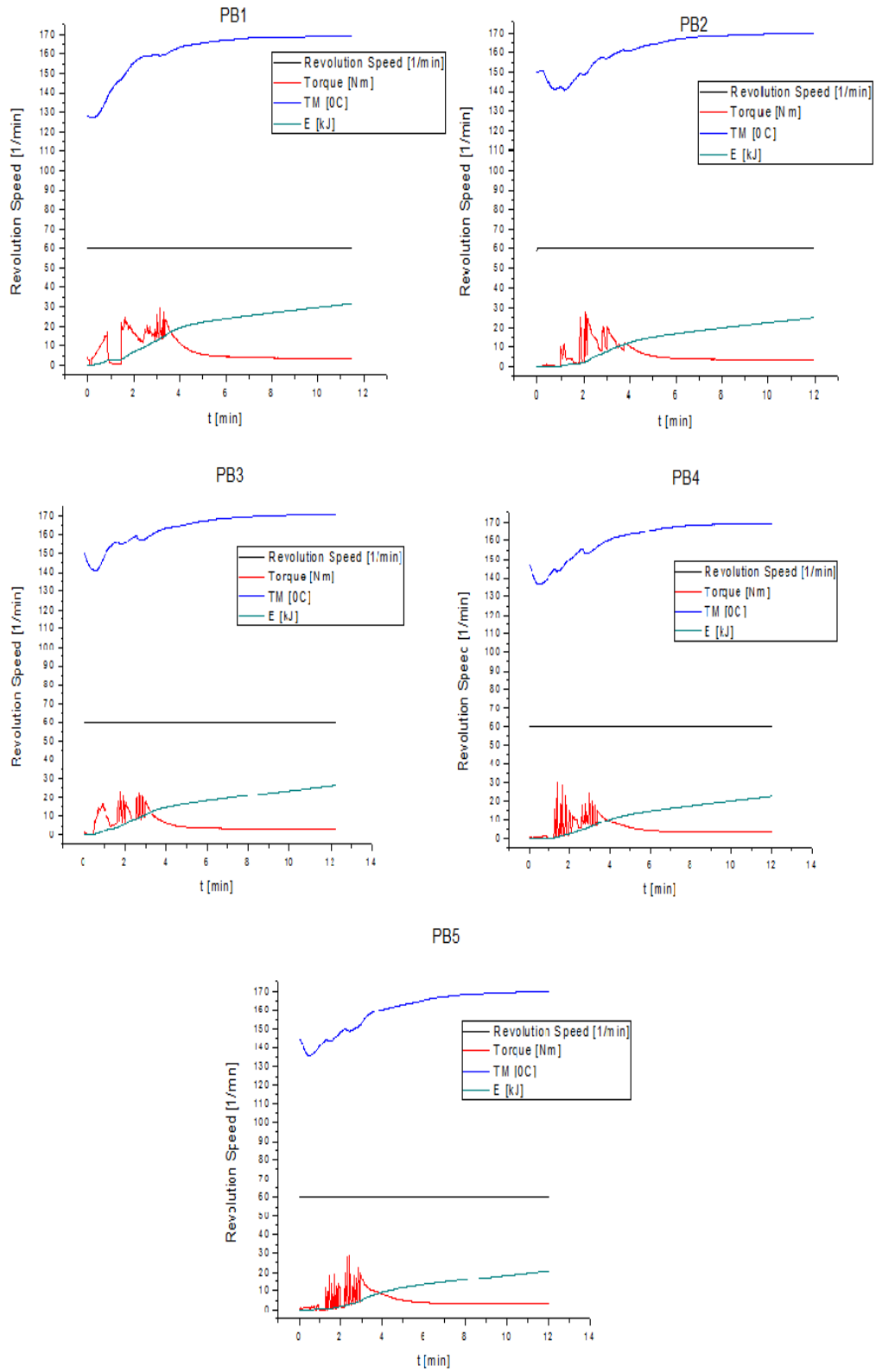


Figure 4.4: Effect on torque by varying BPO content at constant MAH.

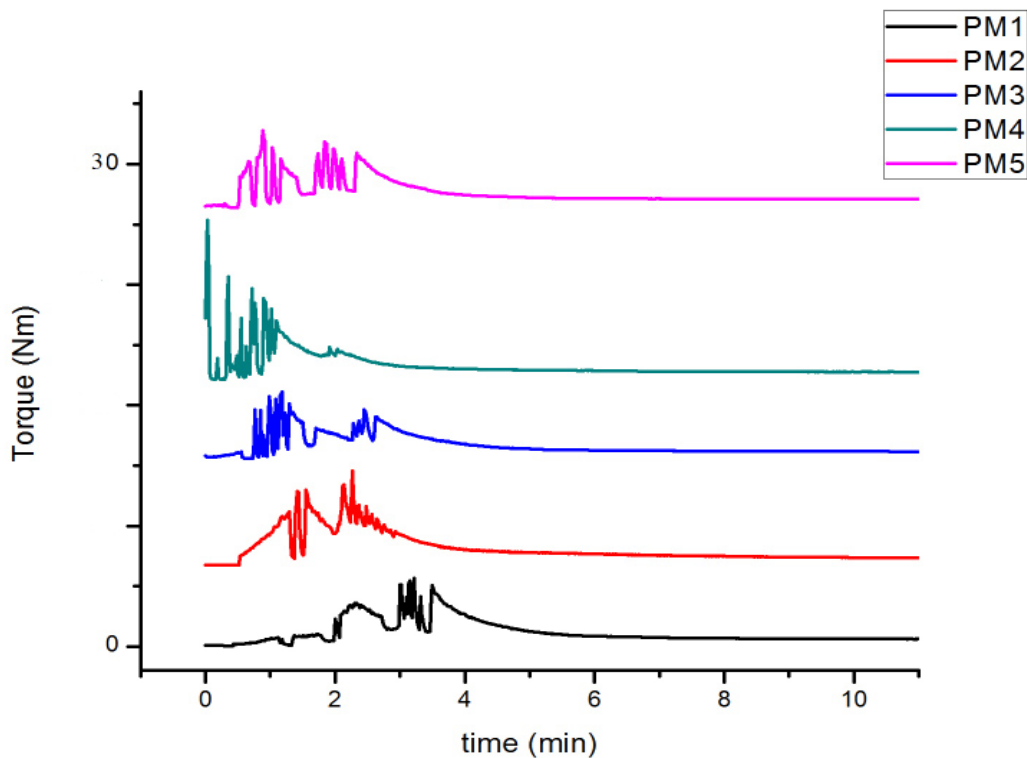


Figure 4.5: Torque variation by altering MAH concentration.

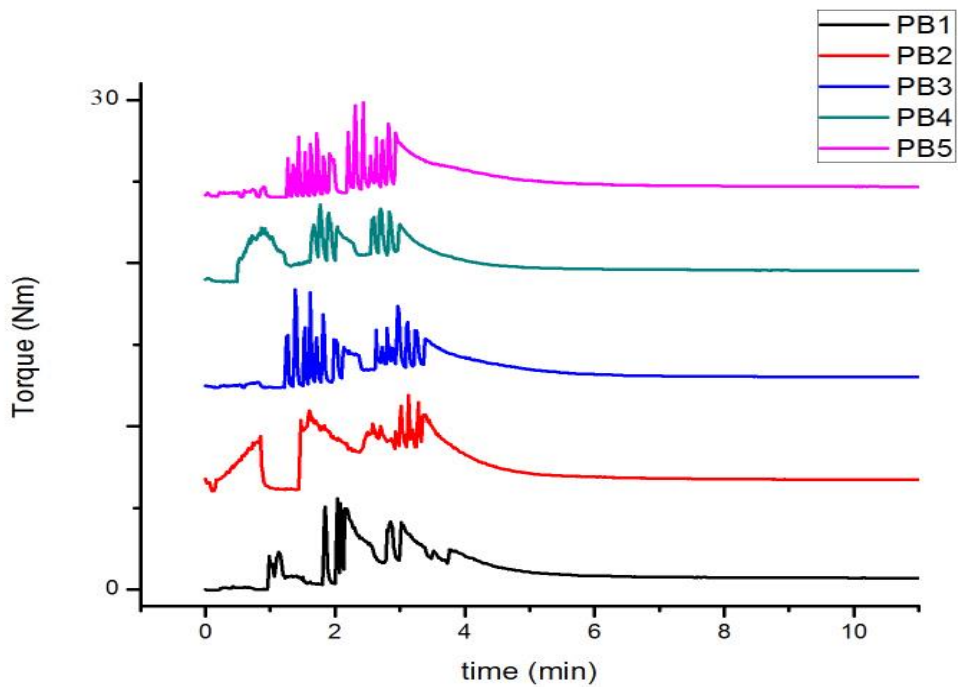


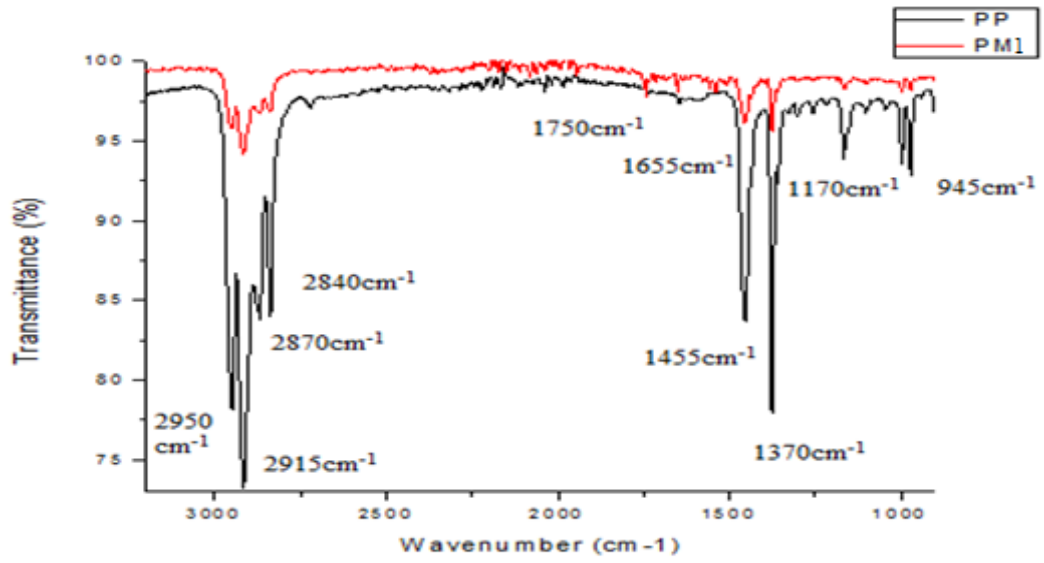
Figure 4.6: Torque variation by altering BPO concentration.

4a.2: FTIR Analysis of Grafted PP Samples

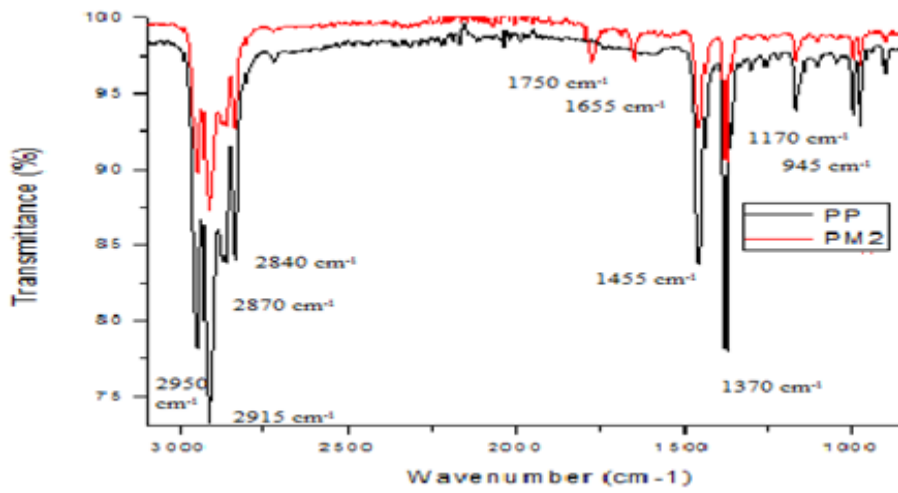
FTIR spectra of pure PP and MAH grafted PP with varying MAH and BPO content are shown in figure 4.7 and 4.8 respectively. In all spectra, pure and grafted, there are peaks at 2950 cm^{-1} for the asymmetric stretching of methyl group ($-\text{CH}_3$), at 2915 cm^{-1} for the asymmetric stretching of $-\text{CH}_2-$, at 2870 cm^{-1} for the symmetric stretching of methyl group ($-\text{CH}_3$), at 2840 cm^{-1} for the symmetric stretching of $-\text{CH}_2-$, bending peaks of $-\text{CH}_2-$ and $-\text{CH}_3$ are at 1455 cm^{-1} and 1370 cm^{-1} respectively. In all grafted samples, two peaks appeared on 1750 cm^{-1} for carbonyl group ($\text{C}=\text{O}$) of five membered ring anhydride and 1655 cm^{-1} for $\text{C}=\text{C}$. These peaks confirmed the presence of MAH grafted PP chains along with pure PP. For all MAH grafted samples, FTIR spectra displayed reduction in absorbance for CH stretching and bending. This is due the change in dipole moment after grafting MAH on PP. Peak at 1170 cm^{-1} is of C-H in plane deformation and at 945 cm^{-1} is due to C-H out of plane deformation. Carbonyl index was calculated for all grafted samples by using equation 10. Table 4.1 displays CI values for all samples. CI value is directly proportional to MAH grafting. Higher CI value relates to high grafting.

Table 4.1: CI values of all grafted samples

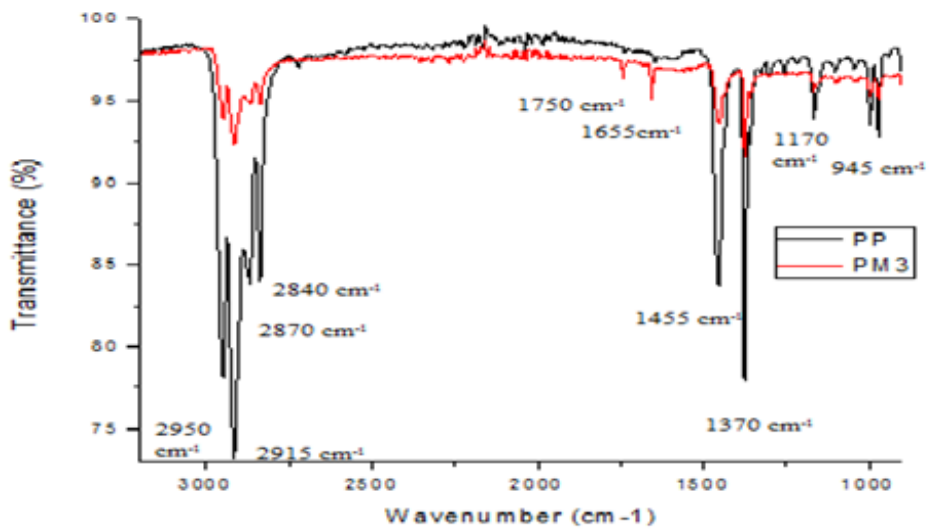
Sample Name	MAH (phr)	BPO (phr)	Carbonyl Index (CI)	Sample Name	MAH (phr)	BPO (phr)	Carbonyl Index (CI)
PM1	0.05	0.4	0.24	PB1	0.15	0.2	0.25
PM2	0.10	0.4	0.37	PB2	0.15	0.3	0.27
PM3	0.15	0.4	0.38	PB3	0.15	0.4	0.38
PM4	0.20	0.4	0.41	PB4	0.15	0.45	0.42
PM5	0.25	0.4	0.40	PB5	0.15	0.5	0.41



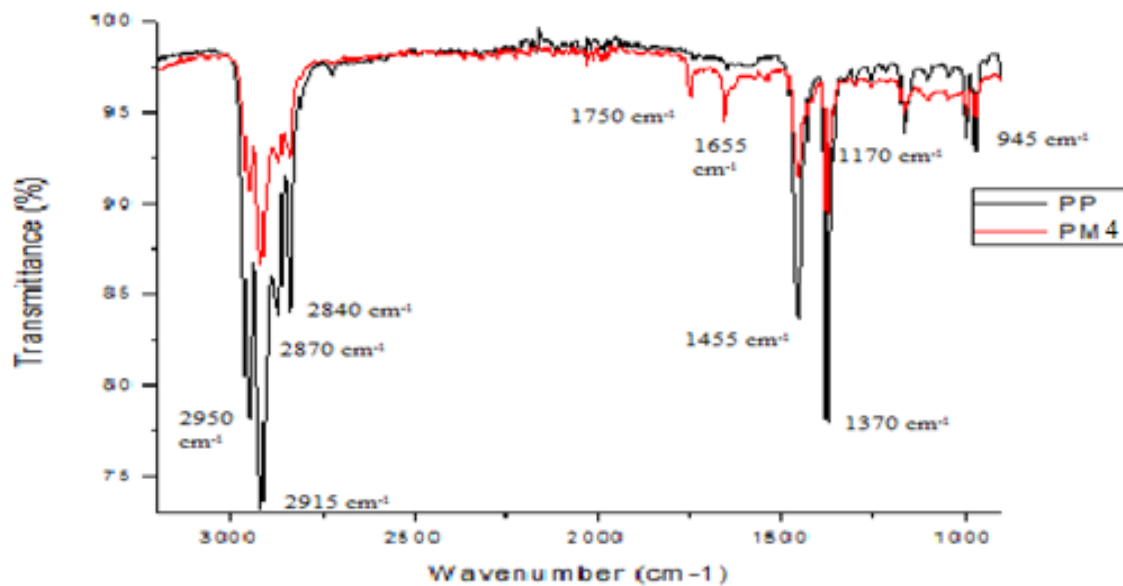
1)



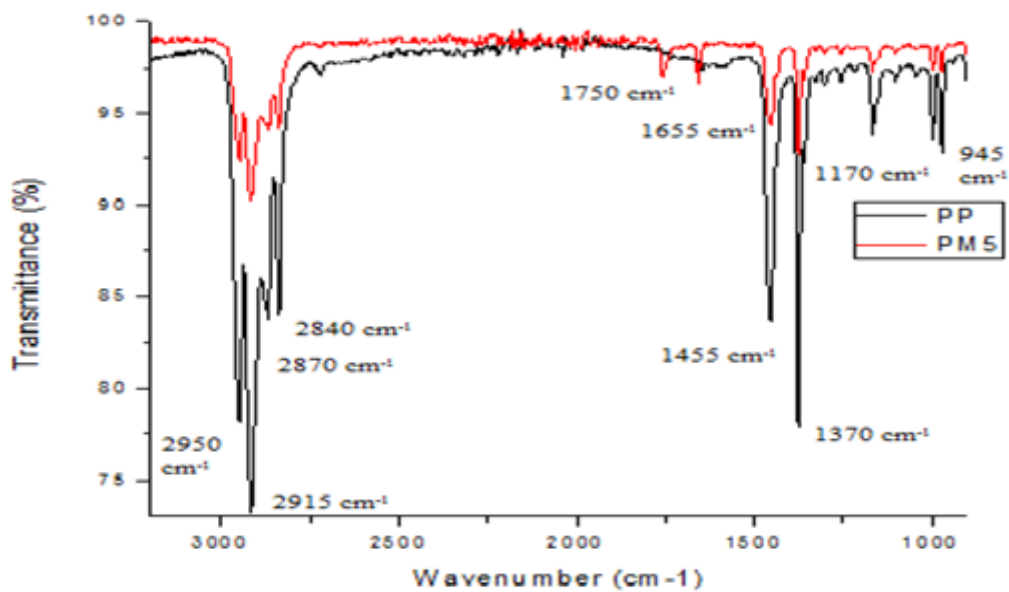
2)



3)

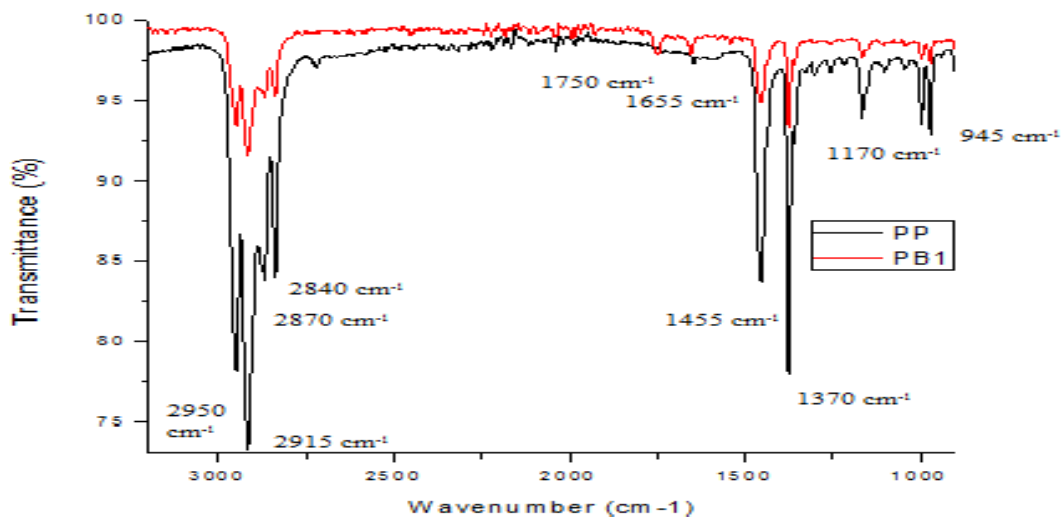


4)

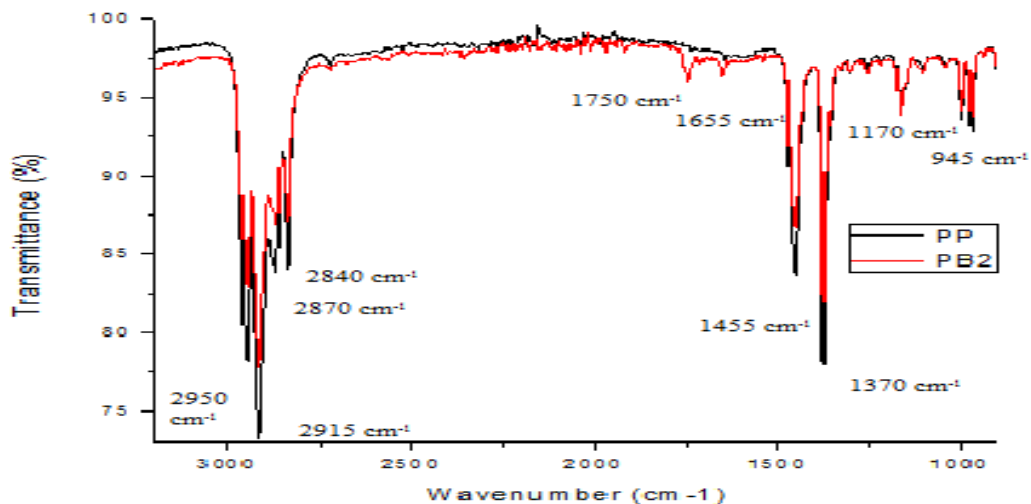


5)

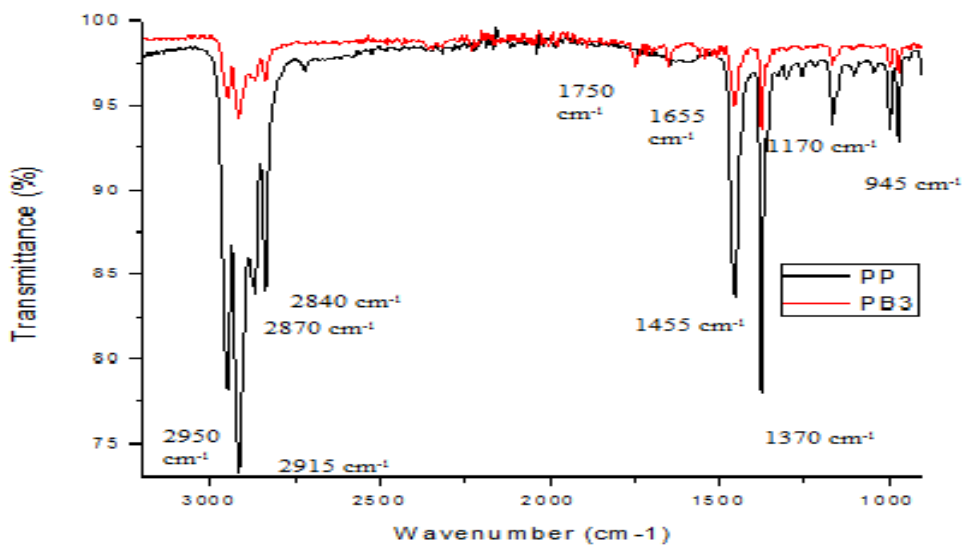
Figure 4.7: FTIR analysis spectra of MAH grafted PP samples by varying MAH content (from 1 to 5) in comparison of pure PP spectra.



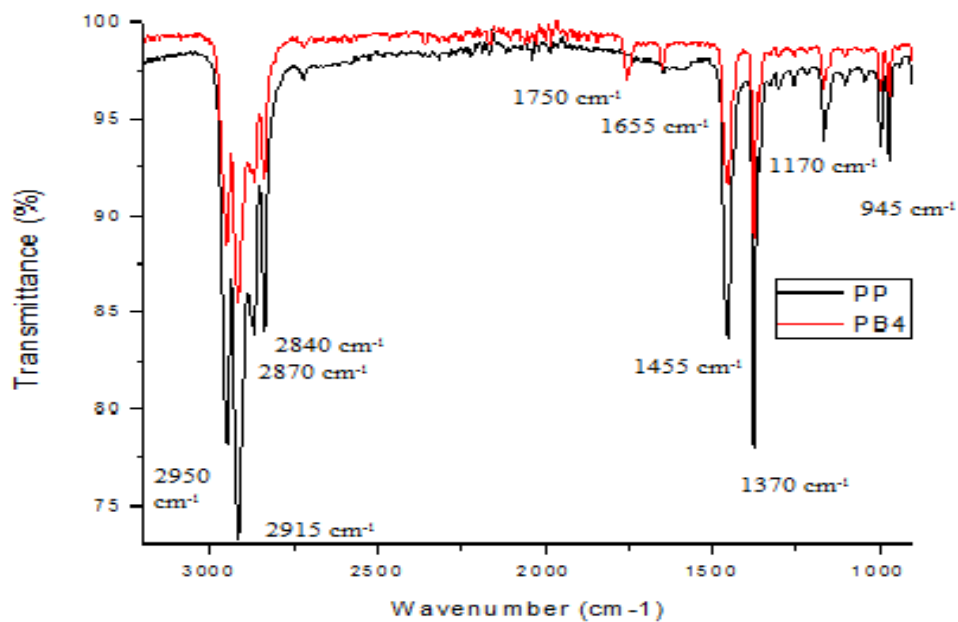
1)



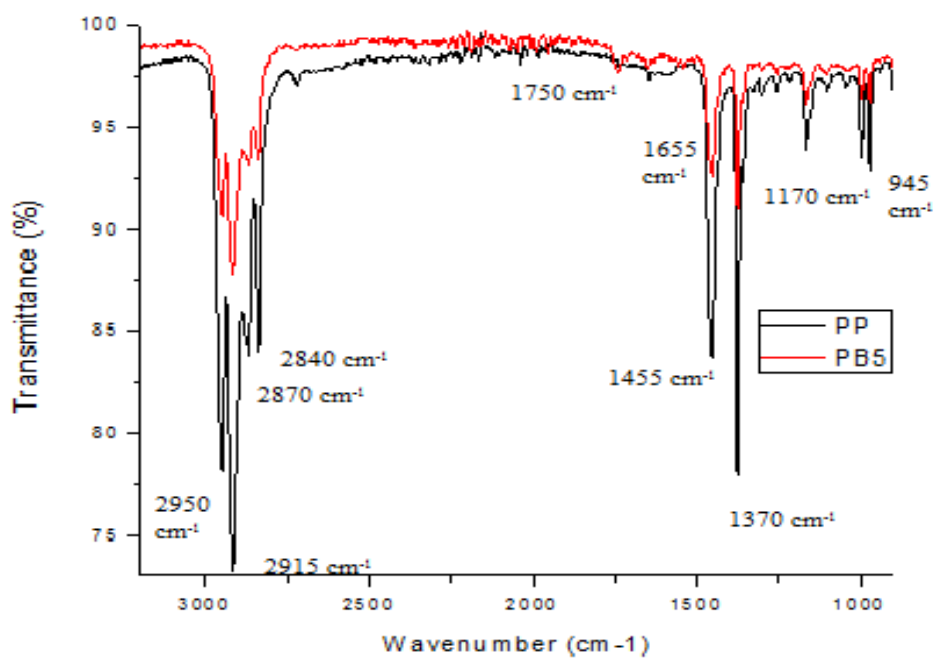
2)



3)



4)



5)

Figure 4.8: FTIR analysis spectra of MAH grafted PP samples by varying BPO content (from 1 to 5) in comparison of pure PP spectra.

4a.3: Thermal Analysis of Grafted Samples

Thermal properties of functionalized PP including melting temperature and percentage crystallinity was analysed by DSC thermograms. A comparison of all processed samples by reactive extrusion with varying MAH and BPO contents are shown in figure 4.9 and figure 4.10 respectively. All grafted samples showed high fusion enthalpy. Percentage crystallinity of processed samples was calculated by equation 11, variation in percentage crystallinity and melting temperature by different MAH and BPO contents for grafted PP are also exhibited in figure 4.11 and figure 4.12 respectively. By analysing these effects it can be deduced that in all processed samples percentage crystallinity was much increased, owing to the degradation of PP chains into shorter chains by the addition of BPO and MAH. Chain scission caused reduction in molecular weight and further reduced entanglements in chains, this reduction raised the degree of order of PP chains and hence caused an increase in overall crystallinity. [71]

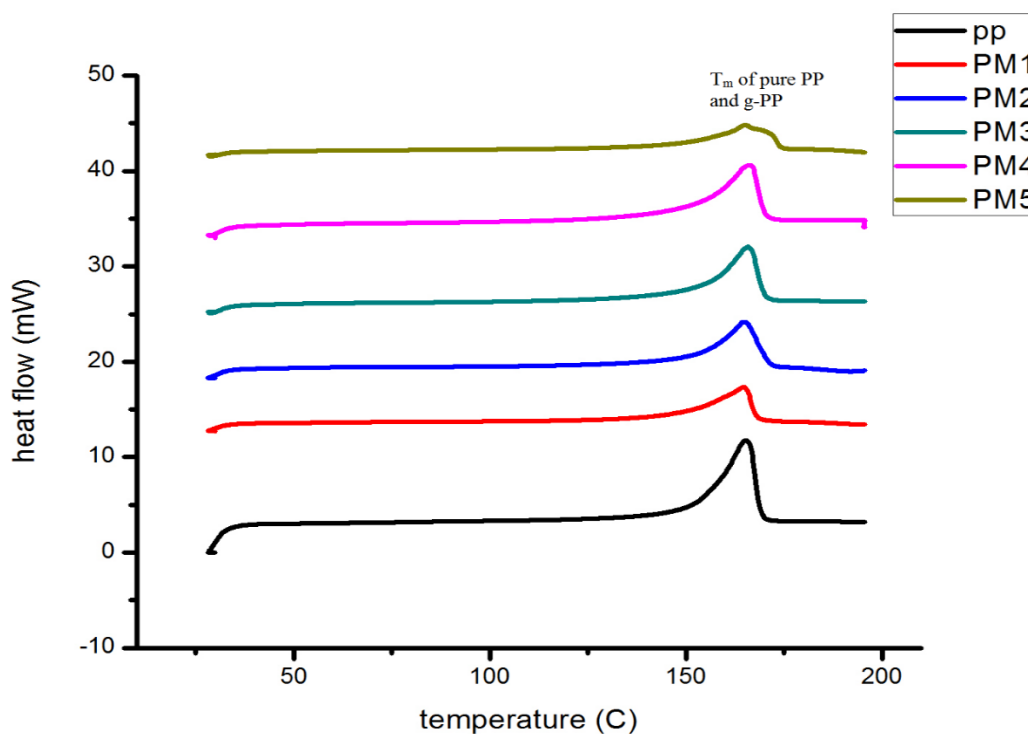


Figure 4.9: Differential scanning calorimetry (DSC) thermograms for MAH grafted PP samples for varying MAH contents.

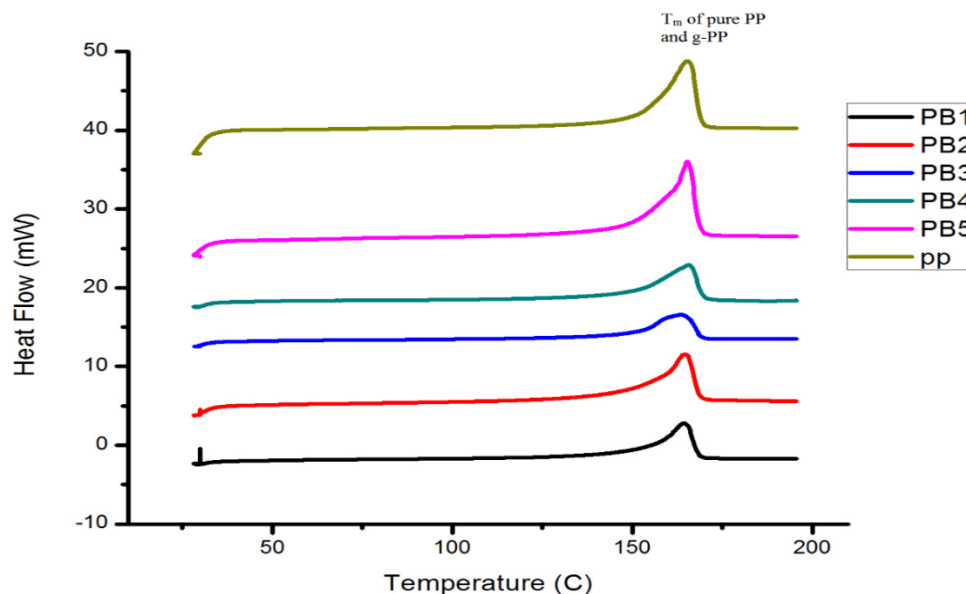


Figure 4.10: Differential scanning calorimetry (DSC) thermograms for MAH grafted PP samples for varying BPO contents.

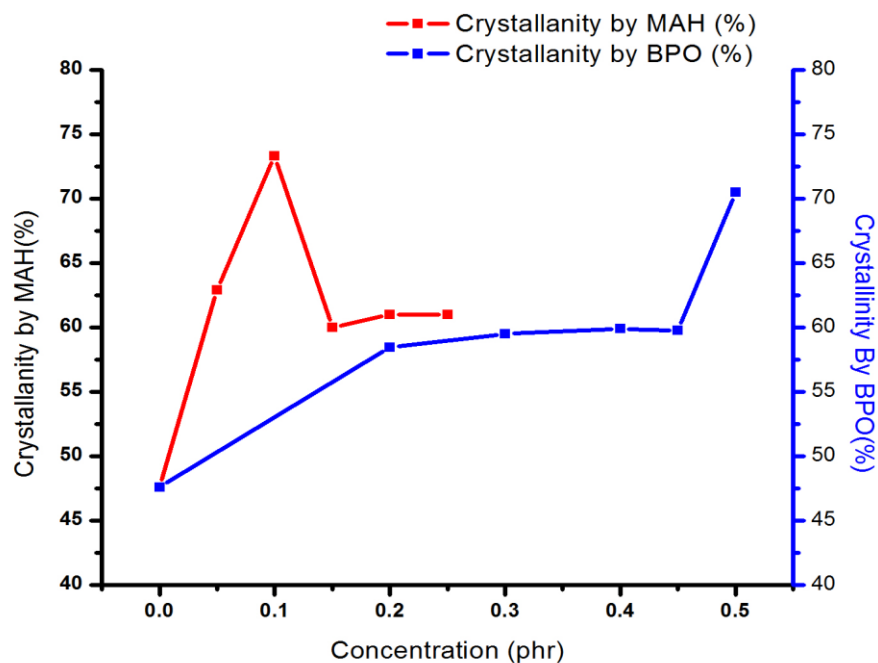


Figure 4.11: Effect on percentage crystallinity for grafted samples by varying MAH and BPO content.

When BPO content was raised, chains scission was increased due to high level of degradation and thus percentage crystallinity remained high for all samples. On contrary,

when MAH concentration was increased at 0.1 phr, percentage crystallinity reduced and with further addition of MAH % crystallinity remained unaffected. The reason for the slight fall after 0.1 phr MAH was due to complex molecules formation leading to hindrance in chains' packing. [80]

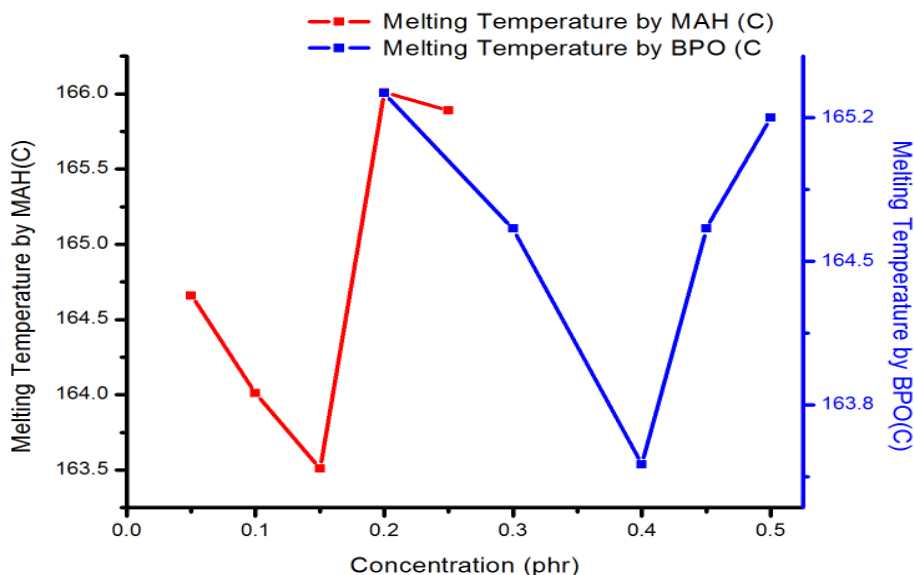


Figure 4.12: Effect on Melting Temperature (T_m) for grafted samples by varying MAH and BPO contents.

The structural changes caused by adding maleic anhydride on PP chains also influenced melting temperature to some extent. Variation in MAH at constant BPO and in BPO at constant MAH, first reduced melting temperature of processed samples and then a sudden rise was detected. The fall in T_m at low concentrations of MAH and BPO was owing to the chains breakage and branching on main chain. But at high amount of MAH and BPO complex molecular structures formed and melting temperature increased. [71, 80]

4a.4: Melt Flow Index (MFI)

MFI values for all functionalized polypropylene samples are displayed in table 4.2 below. Figure 4.13 displays that by adding low content of MAH and BPO, MFI value increase remarkably. This was confirmed from literature[71, 81]. By adding MAH and

BPO polymer chain scission occur due to termination by chain transfer not by combination.

Table 4.2: Melt Flow Index for all processed samples and pure polypropylene.

Sample Name	MFI (g/10min) at 2.16 kg and 190° C	Sample Name	MFI (g/10min) at 2.16 kg and 190° C
PP	3.297	PB1	11.84
PM1	6.011	PB2	13.99
PM2	9.256	PB3	15.97
PM3	13.28	PB4	12.70
PM4	8.901	PB5	8.380
PM5	8.604	PB1	11.84

It can be infer that combination reaction for termination is less probable than chain transfer. Shorter chains with low molecular weight causes high flow rate. But as the amount of MAH and BPO increases further, complex molecules form this will lower its MFI values.[71]

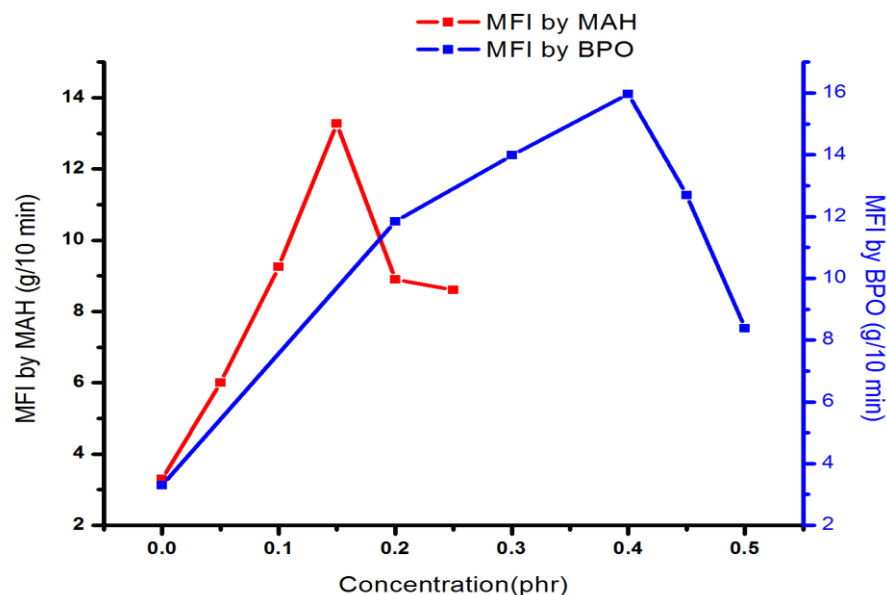


Figure 4.1: Melt Flow Index of functionalized samples by varying MAH and BPO

4b: Results and Discussion of Blended Films

4b.1: Fourier Transform Infrared Spectroscopy (FTIR)

FTIR spectra of pure PP, pure PET and MAH-g-PP/PP/PET blend shows many alterations presented in figure 4.14. In MAH-g-PP/PP/PET blend there is a weak broad band of OH at about 3600 cm^{-1} due to water absorption. Four adjacent stacks at 2950 cm^{-1} for the asymmetric stretching of methyl group ($-\text{CH}_3$), at 2915 cm^{-1} for the asymmetric stretching of $-\text{CH}_2$, at 2870 cm^{-1} for the symmetric stretching of methyl group ($-\text{CH}_3$), at 2840 cm^{-1} for the symmetric stretching of $-\text{CH}_2-$, bending peaks of $-\text{CH}_2-$ and $-\text{CH}_3$ are at 1455 cm^{-1} and 1370 cm^{-1} respectively are present in pure PP and -MAH-g-PP/PET blend but is not visible in pure PET. In pure PET and MAH-g-PP/PP/PET blend samples, peak appeared on 1750 cm^{-1} for carbonyl group ($\text{C}=\text{O}$). A strong peak at 1250 cm^{-1} which is clear in pure PET and much strong in MAH-g-PP/PP/PET blend confirms the presence of ester linkage ($\text{C}-\text{O}-\text{C}$). [67]

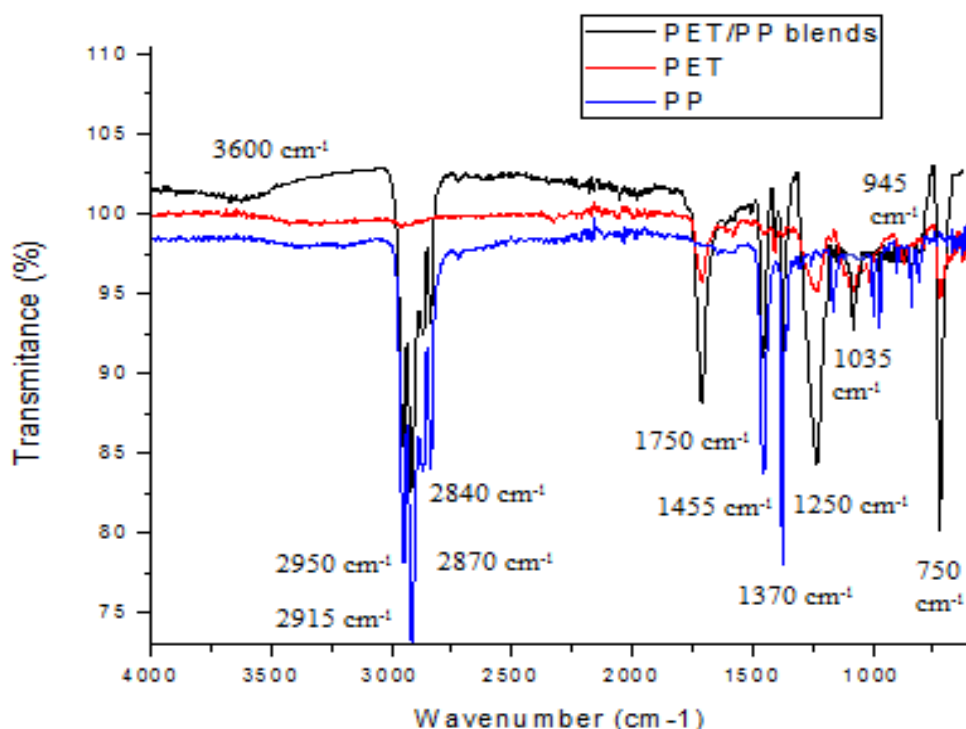


Figure 4.14: FTIR spectra comparison between pure PP, pure PET and MAH-g-PP/PP/PET.

In fingerprint region there is peak in PET and blend spectra at 1035 cm^{-1} due to C-O stretch. A much sharp peak at 750 cm^{-1} in pure PET and blend is of benzene ring. There was no prominent shift in peaks that confirms the absence of any bonding between PET and PP in the blend.

4b.2: Thermal Analysis by Differential Scanning Calorimetry (DSC)

DSC thermogram of MAH-g-PP/PP/PET blend is displayed in figure 4.15. From DSC results it was deduced that glass transition temperature (T_g) of PET appeared at $82\text{ }^\circ\text{C}$ but in the blend with compatibilizer T_g was not detectable and there might be possibilities that T_g was not changed. [82]

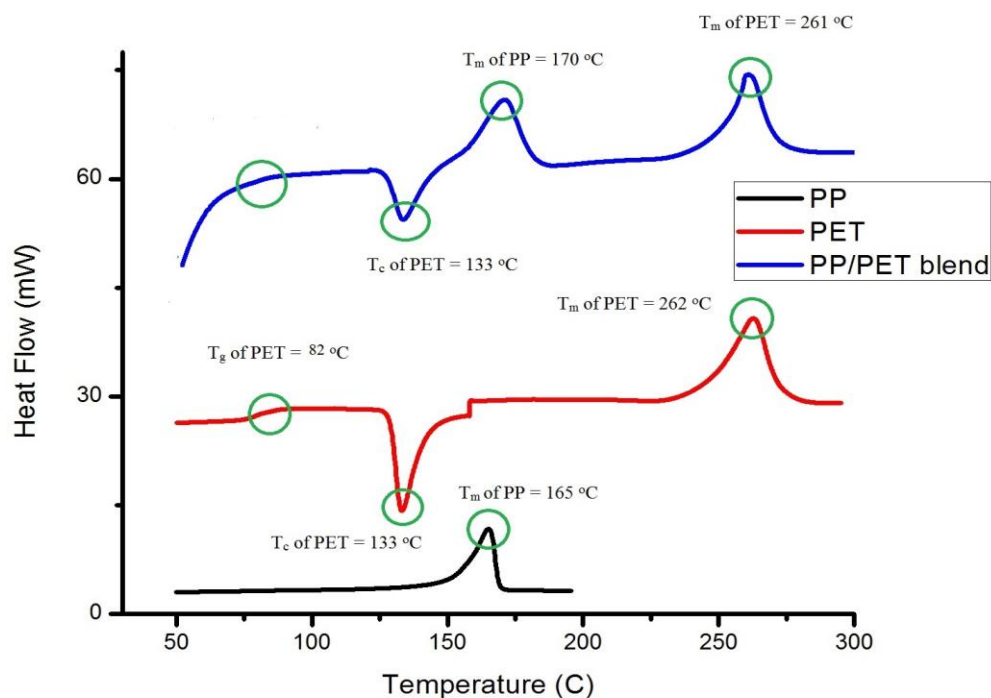


Figure 4.15: DSC thermogram of MAH-g-PP/PP/PET blend, PP and PET

T_m of PP in the blends was increased from $165\text{ }^\circ\text{C}$ to $170\text{ }^\circ\text{C}$ compare to pure PP due to reason that addition of PET in PP effected that chains behaviour. Inside the blends the polymer in majority (PET) started to form coil like structure around the polymer in less amount (PP), this chains behaviour demanded high temperature for the melting of PP. [83]

There was no effect on the crystallization temperature of PET in the compatibilized blends. T_m of PET was not changed by blending with PP. In PET/PP blend without compatibilizer displayed in figure in 4.16, T_g of blend without compatibility was also not detectable.[82, 83]

T_m of PET in the blend was almost same and T_m of PP was high in uncompatibilized blend because of coiling of PET around PP. T_c of PET was observed to be decrease due the coursing of crystals that will form at low temperature in blend compare of pure PET in which well-shaped crystals form at high temperature. Thermal properties were overall improved by adding compatibilizer as first melting appears at higher temperature than pure PP and PET/PP blend without compatibilizer.

Heat of fusion of PP in the blend was not highly effected but heat of fusion of PET in the blend was decreased shown in figure 4.17 and hence crystallinity of PET was low calculated by equation 11. This decrease was because of hindrance created by interactions generated after blending. Table 4.3 displays the variation in % crystallinity of PET after blending.

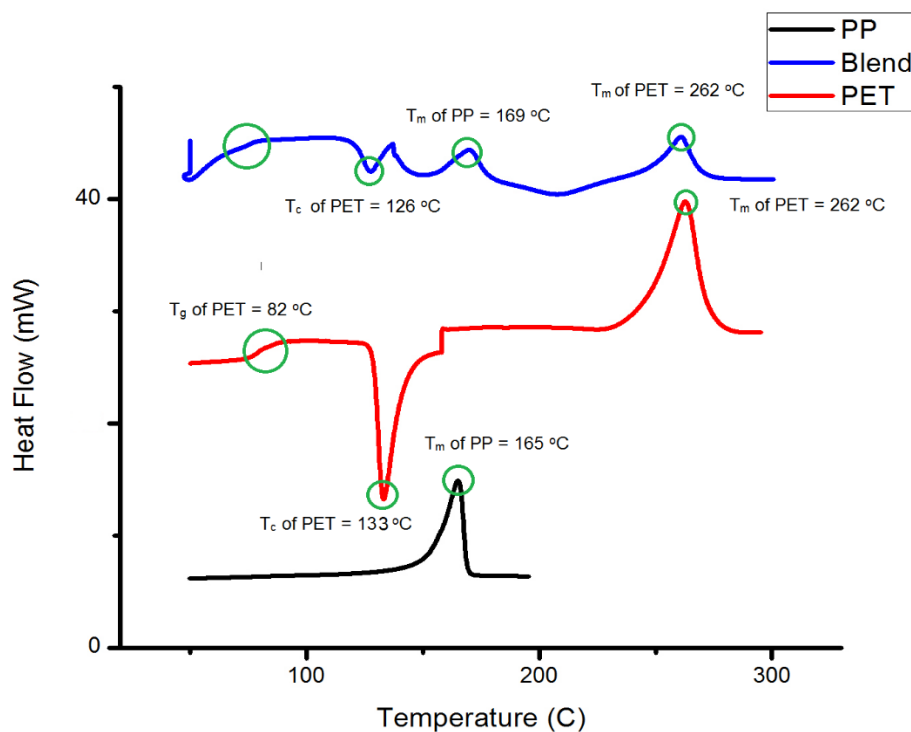
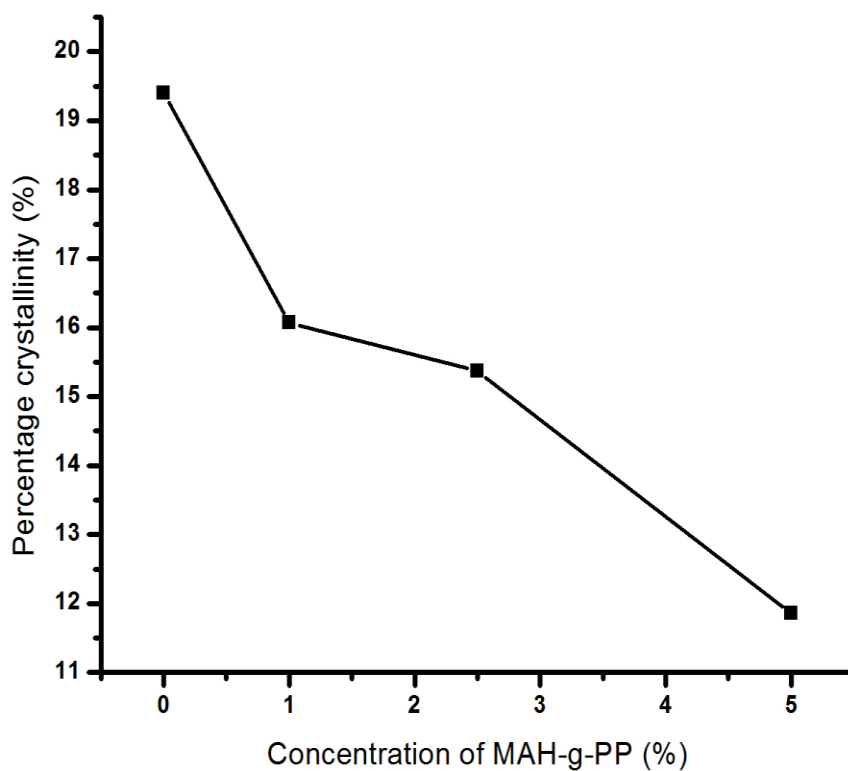


Figure 4.16: DSC thermogram of /PP/PET blend, PP and PET

Table 4.3: Percentage crystallinity of PET in the blend.

Compositions	% Crystallinity of PET
CB1	16.07
CB2	15.37
CB3	11.86
CB4	19.40
CB5	27.85
CB6	-

*Figure 4.17: Percentage crystallinity of blends of different composition.*

4b.3: Morphology by Scanning Electron Microscopy (SEM)

Figure 4.18 displays the scanning electron microscopy images of pure PP and PET and figure 4.19 shows the images of compatibilized and noncompatibilized PP/PET blends. From the images we can analyse that pure PET and pure PP has completely uniform microstructure and from the morphology of the blends the compatibility between PET and PP can be seen.

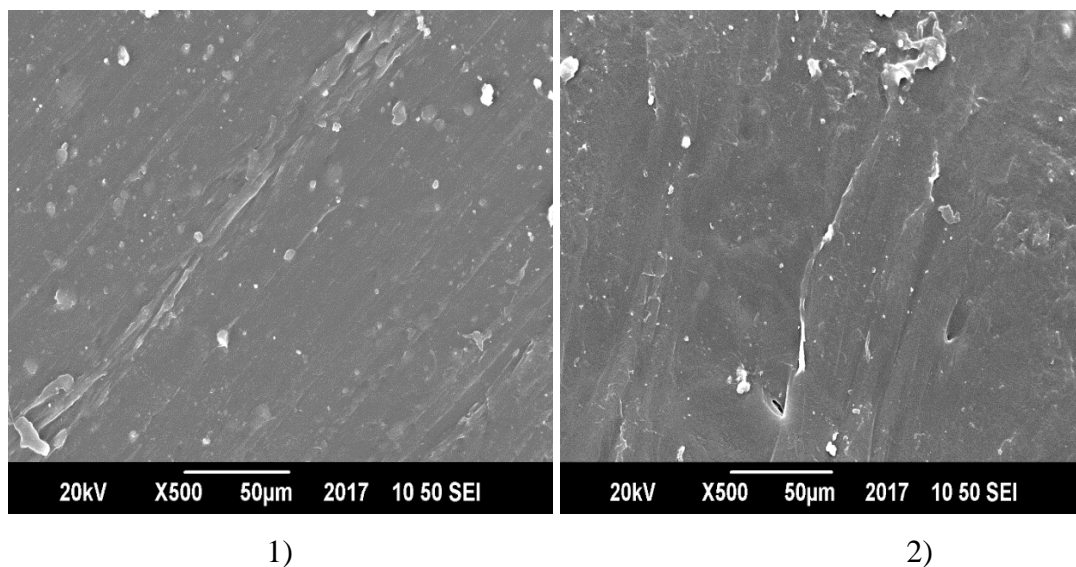


Figure 4.18: SEM images of 1) pure PET and 2) pure PP

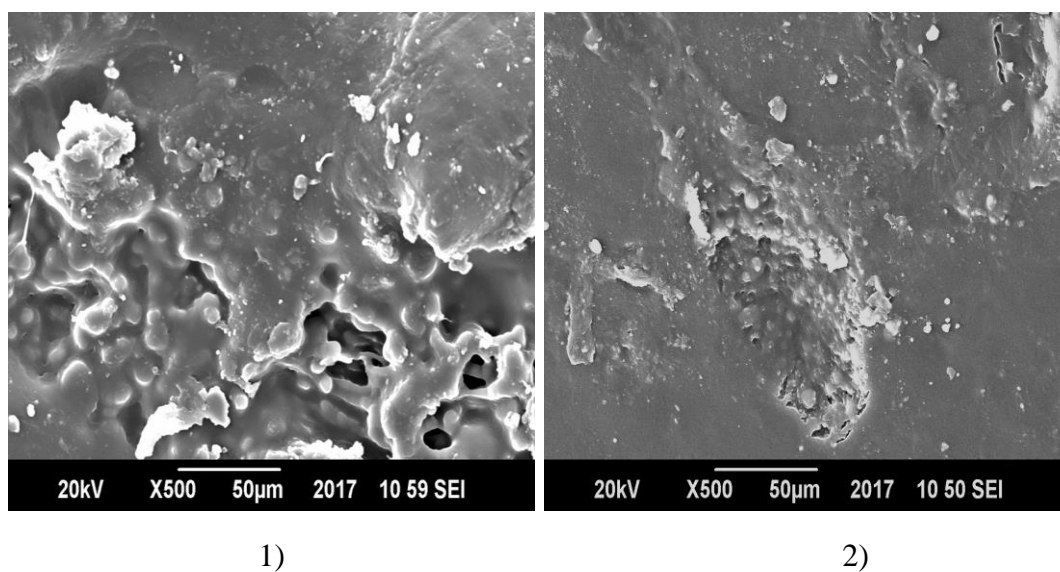


Figure 4.19: SEM images of 1) PP/PET and 2) MAH-g-PP/PP/PET blends with composition 40/60 and 2.5/37.5/60 respectively.

The presence of MAH-g-PP in blends promoted the formation of much finer dispersed morphology, uniformity and much better adhesion than noncompatibilized blends. This increase in fineness of the blend resulted in reduction of voids and hence it reduced the passage of molecules through the films and decrease its permeability for water molecules. Figure 4.20 and 4.21 are the details of compatibilized blends. [68, 69, 84]

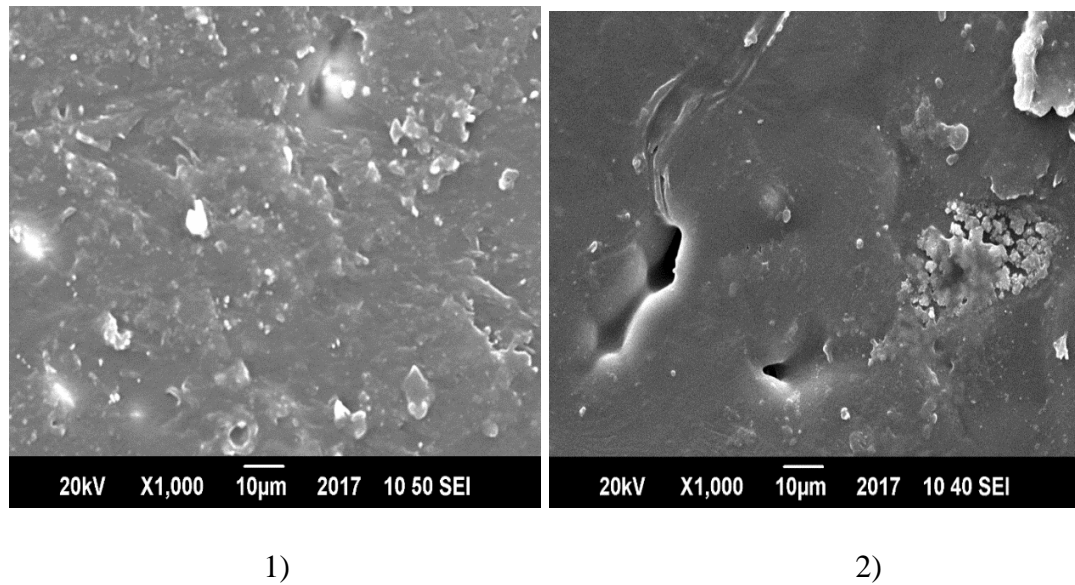


Figure 4.20: SEM images of 1) MAH-g-PP/PP/PET and 2) MAH-g-PP/PP/PET blends with composition 2.5/39/60 and 5/35/60 respectively.

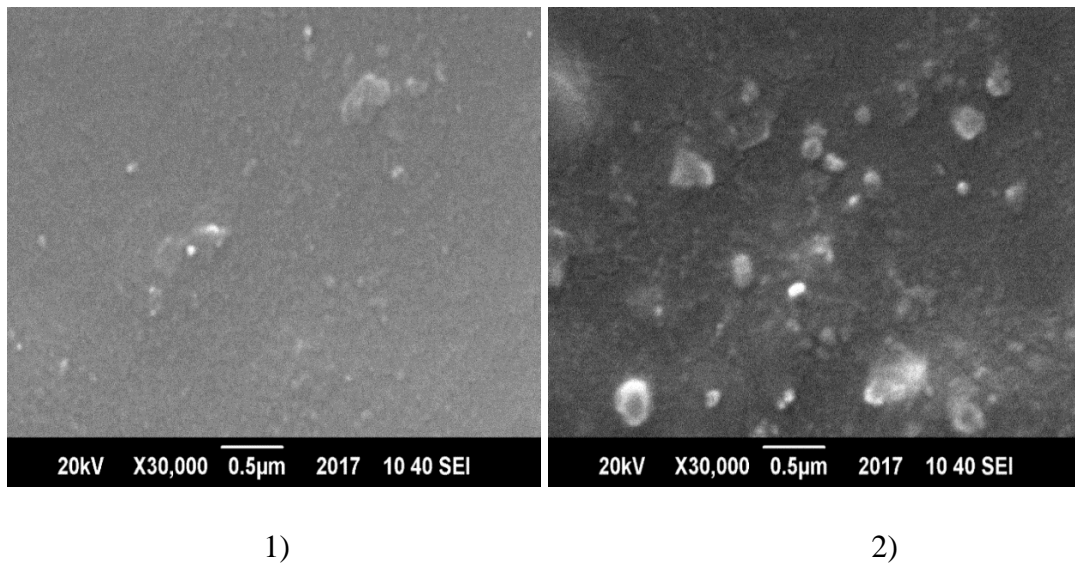


Figure 4.21: SEM images of 1) MAH-g-PP/PP/PET and 2) MAH-g-PP/PP/PET blends with composition 1/39/60 and 2.5/37.5/60 respectively.

In figure 4.20 SEM image of 5% compatibilizer showed some voids that are probably due to uneven physical interactions between the two polymers. In blend of 2.5 % and 5 % compatibilizer, there are agglomerates that showed immiscibility of PET and PP at some areas in the blend. PET molecules started to join with each other due to greater interactions between same types of molecules to stabilize system. [85]

Fracture analysis of blends was also done by SEM images explained in figure 4.22. The spherical shaped beads belonged to PP polymer and the main matrix is PET. These spherical beads are clearly seen to be debounded from the matrix material due to the lack of interfacial adhesion in uncompatibilized blend. A large number of holes are clearly visible in non compatibilized samples owing to the pull out of these weakly adhered polymers. Functionalized PP/PET blends' morphology showed a smaller particle size due to greater interaction. Spherical shaped beads are now seemed to be adhered to the matrix by forming bridges. These interactions are due to dipole-dipole attractions between PET's carbonyl group and maleic anhydride group in PP. In the fractured surface of compatibilized blends we can analyse the fibrils extension as well as plane surface fracture, so it can be illustrated that the functionalized PP/PET is moderately ductile.[68]

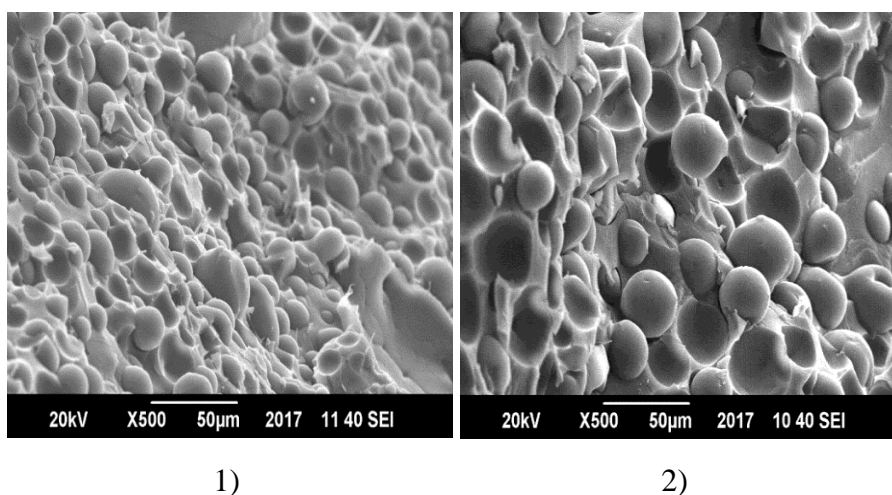


Figure 4.22: SEM images of fracture analysis of 60 % PET 1) 5% MAH-g-PP/PET blends 2) noncompatibilized PP/PET.

The plane surface showed brittle fracture, brittleness in the blended films was due to less alignment and disordered PET chains. Chains were not aligned because of annealing

of blended films at room temperature. Quenching can generate ordered structure with superior mechanical properties.

An optimum amount of compatibilizer can provide homogeneous PET/PP blend with less phase separations. 1% compatibilizer is the amount of MAH-g-PP that showed best blend of PET/PP with reduced agglomerations and voids.

4b.4: Water vapours Permeability

Water vapours' weight loss from the films was detected using ASTM E96 and permeability calculations were done to estimate the permeability of water vapours through the prepared films. Pure PET material has high permeability for water molecules because of its polar nature, it absorbs water. By absorbing high percentage of water molecules, greater diffusion occurs through PET, its weight loss is 1.973 % greater than of pure PP. Diffusion of penetrant molecules depends on the size of molecules, polarity of material, temperature on which diffusion occurs and concentration difference of molecules across the film.

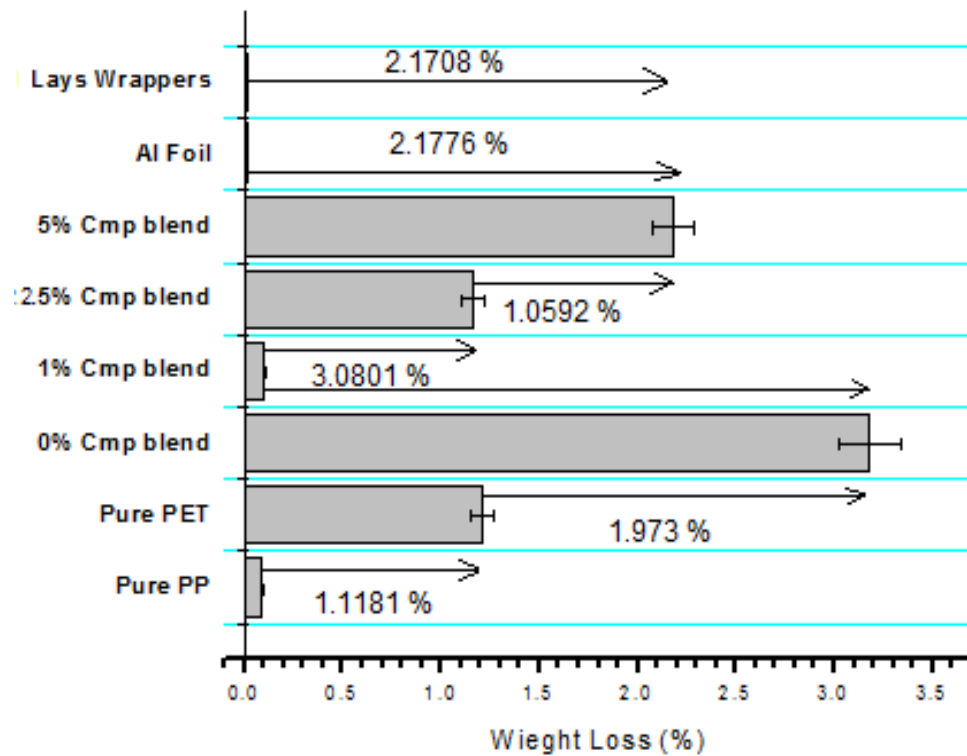


Figure 4.23: Water vapours weight loss of prepared films.

Figure 4.23 compares the blends' WVTR weight loss with pure PP and PET, Aluminium foil and Lays wrapper, it can be deduced that, when PET was blended with PP using 1% compatibilizer, its water resistance improved because of PP matrix that hindered water molecules passage through the films. Compatibilized blend resulted in reduced voids inside the blend and free space available to the water molecules to diffuse through the film decreased. However, at higher percentage of compatibilizer, uneven physical interactions between the PP and PET resulted in voids in the films that will increase water molecules' permeability.

Defects in the film also lower its barrier properties for water molecules. When there is less interaction in the blend, films will not be homogeneous and defective sites will allow the passage of water molecules through the films. At 0 percent compatibilizer, PET and PP were completely phase separated analysed by SEM images. High weight loss that was 1.9370 % greater than pure PET, was detected in the noncompatibilized films attributed to defects and voids in heterogeneous blend.

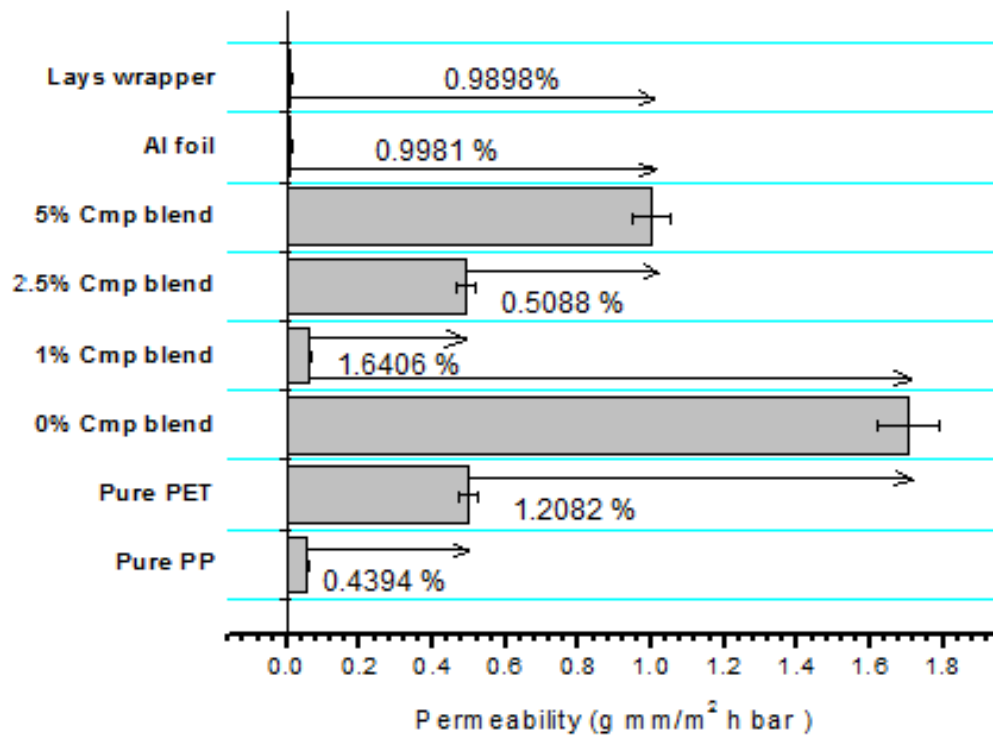


Figure 4.24: Water vapours permeability of prepared films.

Water vapours permeability calculated according to ASTM E-96 is displayed in figure 4.24. These results shows high permeation of water for uncompatibilized blend that was 1.2082 % greater than pure PET and at higher value of compatibilizer also. High permeability for water molecules is due to voids and defects in the films. It can be illustrated from above results that 1 percent MAH-g-PP is the optimum value of compatibilizer in PET/PP blend which showed permeability of water nearly equal to pure PP and also very small difference than conventional lays wrapper. Water vapours transmission rate increased in other blends because of no compatibility and less physical interactions between polymers. Hence, it is concluded that addition of compatibilizer in an optimum amount in PET/PP blend improved the water vapour resistance of PET resin by blending. Without compatibilizer PET/PP blend is not useable for food packaging application

Conclusions

- The summary of this work therefore is that reactive extrusion process was successfully carried out for tailor made compatibilizer of MAH grafted onto PP (MAH-g-PP).
- MAH grafted carbonyl groups resulted in carbonyl index values, and highest value of 0.41 was observed at 0.2 phr MAH and 0.4 phr BPO.
- Viscosity was detected to be low by analysing torque with grafting MAH on PP that make the processing easier. Greater amount of MAH and BPO from an optimum value will lower material's properties. After grafting PP by MAH, MFI and crystallinity was much increased due to short chains and less entanglement.
- MAH-g-PP can be used as compatibilizer to make a homogeneous blend of PET and PP. 1% Compatibilizer in 60/40 PET/PP blend seems to provide best homogeneous blends relative to other concentrations.
- Thermal resistance of blends was improved by adding PP in PET, melting of blend started at 170 °C. Processing temperature of blend was 200 °C resulted in ease in processing of PET.
- 1% Compatibilizer in 60/40 PET/PP blend gave less voids, defect free structure and high thermal properties. Plastic films exhibited excellent lower permeability for 1% compatibilizer in 60/40 PET-PP blends. Concentration of compatibilizer greater than 1 % provides defects in the film that eventually allow the passage of water vapours molecules.
- More than 1% compatibilizer in blend generated uneven physical interactions in the blend, owing to these defects in the films appeared that showed a high permeability for water molecules through the films. So it can be concluded that 1% MAH-g-PP provided a blend with combination of properties required in food packaging.

Suggestions for Future Work

- Work can be done to improve the orientation of chains in the blend that will influence on its mechanical properties.

CONCLUSION AND FUTURE WORK

- Further reactive processing parameters can be investigated such as type of free radical, RPM, temperature profiles, additives types and concentrations, and resins including recycled ones
- Further applications of the developed compatibilizer can be explored for various applications such as co-extrusion packaging, adhesives, gases permeability, etc.
- Functionalization of PP by acrylic acid and its blend with PET.
- Oxygen permeability of PET/PP blends using commercial available equipment.

References:

- [1] L. A. Utracki, *Polymer Blends*: Rapra Technology Limited, **2000**.
- [2] A. I. Isayev, *Encyclopedia of Polymer Blends: Volume 1: Fundamentals*: John Wiley & Sons, **2010**.
- [3] V. Thirtha, R. Lehman, and T. Nosker, "Glass transition effects in immiscible polymer blends," in *Proceedings of the Society of Plastics Engineers, ANTEC Conference, Boston*, **2005**, pp. 303-307.
- [4] M. Aubin and R. E. Prud'Homme, "Tg-Composition analysis of miscible polymer blends," *Polymer Engineering & Science*, vol. 28, pp. 1355-1361, **1988**.
- [5] S. S. Yuki Kohno, Yongjun Men, Jiayin Yuan and Hiroyuki Ohno, "Thermoresponsive polyelectrolytes derived from ionic liquids," *Polymer Chemistry*, pp. 2163-2178, .
- [6] D. R. Paul, *Polymer Blends and Mixtures*. London: Martinus Nijhoff Publishers, **1985**.
- [7] L. A. Utracki, *POLYMER BLENDS HANDBOOK*. Netherland: KLUWER ACADEMIC PUBLISHERS, **2002**.
- [8] J. A. Manson, *POLYMER BLENDS AND COMPOSITES*. Pennsylvania,USA: Springer Science, **1976**.
- [9] M. Kryszewski, *POLYMER BLENDS PROCESSING, MORPHOLOGY and PROPERTIES*. Poland: Plenum Press, **1981**.
- [10] Y. W. J.Lange, "Recent Innovations in Barrier Technology for Plastic Packaging " *Packaging Technology and Science*, vol. 16, pp. 149-158, **2003**.
- [11] C. Tzoganakis, "Reactive extrusion of polymers: A review," *Advances in Polymer Technology*, vol. 9, pp. 321-330, **1989**.
- [12] G.-H. Hu, J.-J. Flat, and M. Lambla, "Free-radical grafting of monomers onto polymers by reactive extrusion: principles and applications," in *Reactive modifiers for polymers*, ed: Springer, **1997**, pp. 1-83.
- [13] G. L. Robertson, *Food Packaging Principles and Practice*, Third ed. United States of America: CRC Press, **2012**.

- [14] H. Y. P. Frank A. Paine, *A Handbook of Food Packaging* second ed. Glasgow: Springer Science & Business Media, **1992**.
- [15] *Packaging Technology Series* vol. 5. USA: CRC Press, **2003**.
- [16] J. H. Han, *Innovations in Food Packaging*: Elsevier Science, **2005**.
- [17] J. J. a. F. Kester, O.R., "Edible films and coatings: a review," *Food technology*, vol. 40, pp. 47-59, **1986**.
- [18] S. J. Risch, *Food Packaging: Testing Methods and Applications*: American Chemical Society, **2000**.
- [19] J. K. CAGE, "Introduction to Food Packaging," pp. 3-12.
- [20] S. Alavi, S. Thomas, K. P. Sandeep, N. Kalarikkal, J. Varghese, and S. Yaragalla, *Polymers for Packaging Applications*: Apple Academic Press, **2014**.
- [21] S. E. M. Selke, *Understanding Plastics Packaging Technology*: Hanser Publishers, **1997**.
- [22] V. Stannett, "The transport of gases in synthetic polymeric membranes — an historic perspective," *Journal of Membrane Science*, vol. 3, pp. 97-115, 1978/01/01 **1978**.
- [23] P. J. Corish, *Concise Encyclopedia of Polymer Processing & Applications*: Elsevier Science & Technology Books, **1992**.
- [24] V. Siracusa, "Food Packaging Permeability Behaviour: A Report," *International Journal of Polymer Science*, vol. 2012, p. 11, **2012**.
- [25] P. J. Corish, "Advances in Materials Science and Engineering," in *Concise Encyclopaedia of Polymer Processing & Applications*", ed: The MIT Press, **1992**, p. 493.
- [26] M.KROOK, "Barrier and Mechanical Properties of Montmorillonite/Polyesteramide Nanocomposites," *Polymer Engineering and Science*, vol. 42, pp. 1238–1246, **2002**.
- [27] S. A. Stern, "The "barrer" permeability unit," *Journal of Polymer Science Part A-2: Polymer Physics*, vol. 6, pp. 1933-1934, **1968**.
- [28] M. Alexandre, Dubois, "Polymer-layered silicate nanocomposites: preparation, properties and uses of a new class of materials," *Materials Science and Engineering*, vol. 28, pp. 1-63, 15 June **2000**.

- [29] A. L. Brody, "Food Packaging Technology," *Food Technology*, vol. 57, pp. 52-54, 12 Dec 2003.
- [30] F. UDDIN, "Clays, Nanoclays, and Montmorillonite Minerals," *Metallurgical and Materials Transactions A*, vol. 39, pp. 2804–2814, 24 September **2008**.
- [31] B. K. G. T. Faïza Bergaya, G. Lagaly, *Hand Book of Clay Science*. France: Elsevier, **2006**.
- [32] S. Q. X. Fu, "Polymer–clay nanocomposites: exfoliation of organophilic montmorillonite nanolayers in polystyrene," *Polymer*, vol. 42, pp. 807–813, **2000**.
- [33] P. G. D. Nascimento, "Structure of Clays and Polymer–Clay Composites Studied by X-ray Absorption Spectroscopie," in *Clays, Clay Minerals and Ceramic Materials Based on Clay Minerals*, ed Brazil: InTech, 3 March **2016**, p. 192.
- [34] M. N. a. A. S. N. ARTZI, "EVOH/Clay Nanocomposites Produced by Dynamic Melt Mixing," *Polymer Enigneering and Science*, vol. 44, pp. 1019–1026, **2004**.
- [35] C. L. a. Y.-W. Mai, "Influence of Aspect Ratio on Barrier Properties of Polymer-Clay Nanocomposites," *American Physical Society* vol. 95, **2005**.
- [36] Q. Z. Bo Xu, Yihu Song, Yonggang Shangguan, "Calculating barrier properties of polymer/clay nanocomposites: Effects of clay layers," *Polymer*, vol. 47, pp. 2904–2910, **2006**.
- [37] M. O. Tomotaka Saito, "Polypropylene-based nano-composite formation: Delamination of organically modified layered filler via solid-state processing," *Polymer*, vol. 51, pp. 4238-4242, **2010**.
- [38] N. F. S. Alix, N. Tenn, B. Alexandre, S. Bourbigot, "Effect of Highly Exfoliated and Oriented Organoclays on the Barrier Properties of Polyamide 6 Based Nanocomposites," *The Journal of Physical Chemistry*, vol. 116, pp. 4937–4947, **2012**.
- [39] A. D. A. Ophir, I. Belinsky, S. Kenig, "Barrier and Mechanical Properties of Nanocomposites Based on Polymer Blends and Organoclays," *Applied Polymer Science*, vol. 116, pp. 72–83, **2009**.
- [40] S.-I. H. Jong-Whan Rhim, Chang-Sik Ha, "Tensile, Water Vapor barrier and antimicrobial properties of PLA/nanoclay composite films," *Food Science and Technology*, vol. 42, pp. 612–617, **2009**.

- [41] C. B. V. Vladimirov, A. Vassiliou, G. Papageorgiou, D. Bikiaris, "Dynamic mechanical and morphological studies of isotactic polypropylene/fumed silica nanocomposite with enhanced gas barrier properties," *Composites Science and Technology*, vol. 66, pp. 2935-2944, **2006**.
- [42] H.-D. Huang, P.-G. Ren, J. Chen, W.-Q. Zhang, X. Ji, and Z.-M. Li, "High barrier graphene oxide nanosheet/poly(vinyl alcohol) nanocomposite films," *Journal of Membrane Science*, vol. 409–410, pp. 156-163, 8/1/ **2012**.
- [43] A. A. A. a. C. W. M. Hyunwoo Kim, "Graphene/Polymer Nanocomposites," *Macromolecules*, vol. 43, pp. 6515–6530, **2010**.
- [44] K. Kalaitzidou, H. Fukushima, and L. T. Drzal, "Multifunctional polypropylene composites produced by incorporation of exfoliated graphite nanoplatelets," *Carbon*, vol. 45, pp. 1446–1452., **2007**.
- [45] G. L. Robertson, *Food Packaging Principles and Practice*. France: CRC Press, **2013**.
- [46] P. J. K. C. F. Struller, N. J. Copeland and C. M. Liauw, "Aluminum oxide barrier layers on polymer web," *Surface and Coatings Technology*, vol. 241, pp. 130–137, **2014**.
- [47] B. M. H. A.P. Roberts, A.P. Sutton, C.R.M. Grovenor, T. Miyamoto , M. Kano , Y. Tsukahara , M. Yanaka, "Gas permeation in silicon-oxide/polymer (SiO_x/PET) barrier films: role of the oxide lattice, nano-defects and macro-defects," *Journal of Membrane Science*, vol. 208, pp. 75–88, **2002**.
- [48] P. Panjan, M. Čekada, M. Panjan, and D. Kek-Merl, "Growth defects in PVD hard coatings," *Vacuum*, vol. 84, pp. 209-214, 8/25/ **2009**.
- [49] M. P. MIKA VÄHÄ-NISSI, ERKKI SALO, JENNI SIEVÄNEN-RAHIJÄRVI, MATTI PUTKONEN and ALI HARLIN, "ATOMIC LAYER DEPOSITED THIN BARRIER FILMS FOR PACKAGING," *CELLULOSE CHEMISTRY AND TECHNOLOGY*, vol. 49, pp. 575-585, **2015**.
- [50] M. C. E. Langereis, S. B. S. Heil, M. C. M. van de Sanden, and W. M. M. Kessels, "Plasma-assisted atomic layer deposition of Al₂O₃ moisture permeation barriers on polymers," *APPLIED PHYSICS LETTERS*, vol. 89, **2006**.

- [51] M. V.-N. Terhi Hirvikorpi, Tuomas Mustonen, Ali Harlin, "Thin Inorganic Barrier Coatings for Packaging Applications," Finland**2010**.
- [52] R. S. M. P. F. Carcia, M. D. Groner, A. Dameron and S. M. George, "Gas Diffusion ultrabarrriers on polymer substrates using Al₂O₃ atomic layer deposition and SiN plasma-enhanced chemical vapor deposition," *Journal of Applied Physics*, vol. 106, **2009**.
- [53] S. E. Citterio C, Testa G, Bonfatti AM, Seves A, "Physico-chemical characterisation of compatibilized poly(propylene)/aromatic polyamide blends," *Macromolecular Materials and Engineering*, vol. 270, pp. 22-27, **1999**.
- [54] G. R. Bhatia A, Bhattacharya and H.S Choi, "Compatibility of biodegradable poly (lactic acid) (PLA) and poly (butylene succinate) (PBS) blends for packaging application," *Korea-Australia Rheology Journal*, vol. 19, pp. 125-131, **2007**.
- [55] A. A. i.-K. J.B. Faisant, M. Bousmina and L. Deschenes, "Morphology, thermomechanical and barrier properties of polypropylene-ethylene vinyl alcohol blends," *Polymer*, vol. 39, pp. 533-545, 18 June **1998**.
- [56] Z. D. Torradas JM, "New laminar oxygen barrier technology for food packaging applications," in *conference proceedings of Society of Plastics Engineers Annual Technical Papers*, Montreal, Canada, **1991**.
- [57] P. S. Nalin Ployetchara, Duangduen Atong and Chiravoot Pechyen, "Blend of polypropylene/poly(lactic acid) for medical packaging application: physicochemical, thermal, mechanical, and barrier properties," *Energy Procedia* vol. 56, pp. 201-210, **2014**.
- [58] M. D. C. a. M. I. Cristina Moniz, "Blends of poly(ethylene terephthalate) and low density polyethylene containing aluminium: A material obtained from packaging recycling," *Journal of Applied Polymer Science* vol. 106, pp. 2524 - 2535 **2007**.
- [59] D. W. Shorten, "Polyolefins for food packaging," *Food Chemistry*, vol. 8, pp. 109-119, **1982**.
- [60] C. Gartner, M. Suárez, and B. L. López, "Grafting of maleic anhydride on polypropylene and its effect on blending with poly(ethylene terephthalate)," *Polymer Engineering & Science*, vol. 48, pp. 1910-1916, **2008**.

- [61] X. Liu, Q. Wu, L. A. Berglund, J. Fan, and Z. Qi, "Polyamide 6-clay nanocomposites/polypropylene-grafted-maleic anhydride alloys," *Polymer*, vol. 42, pp. 8235-8239, 9// **2001**.
- [62] A.-K. A. Faisant JB, Bousmina M, Deschenes L., "Morphology, thermomechanical and barrier properties of polypropylene – ethylene vinyl alcohol blends.," *Polymer*, vol. 39, pp. 533-545, **1998**.
- [63] P. M. Subramanian, "Permeability barriers by controlled morphology of polymer blends," *Polymer Engineering and Science* vol. 25, pp. 483–487, **1985**.
- [64] S. W. K. Dukjoon Kim, "Barrier Property and Morphology of Polypropylene/Polyamide Blend Film," *Korean Journal of Chemical Engineering*, vol. 20, pp. 776–782, **2003**.
- [65] I. B. Valentina Siracusa, Santina Romani, Urtzula Tylewicz, Pietro Rocculi, Marco Dalla Rosa, "Poly(lactic acid)-Modified Films for Food Packaging Application: Physical, Mechanical, and Barrier Behavior," *Journal of Applied Polymer Science* vol. 125, pp. E390–E401, **2012**.
- [66] C. P. Papadopoulou and N. K. Kalfoglou, "Comparison of compatibilizer effectiveness for PET/PP blends: their mechanical, thermal and morphology characterization," *Polymer*, vol. 41, pp. 2543-2555, 3// **2000**.
- [67] H.-T. Chiu and Y.-K. Hsiao, "Compatibilization of Poly(ethylene terephthalate)/Polypropylene Blends with Maleic Anhydride Grafted Polyethylene-Octene Elastomer," *Journal of Polymer Research*, vol. 13, pp. 153-160, **2006**.
- [68] Z. O. Oyman and T. Tinçer, "Melt blending of poly(ethylene terephthalate) with polypropylene in the presence of silane coupling agent," *Journal of Applied Polymer Science*, vol. 89, pp. 1039-1048, **2003**.
- [69] M. Xanthos, M. W. Young, and J. A. Biesenberger, "Polypropylene/polyethylene terephthalate blends compatibilized through functionalization," *Polymer Engineering & Science*, vol. 30, pp. 355-365, **1990**.
- [70] M. Akbari, A. Zadhoush, and M. Haghighat, "PET/PP blending by using PP-g-MA synthesized by solid phase," *Journal of Applied Polymer Science*, vol. 104, pp. 3986-3993, **2007**.

- [71] S. H. P. Bettini and J. A. M. Agnelli, "Grafting of maleic anhydride onto polypropylene by reactive extrusion," *Journal of Applied Polymer Science*, vol. 85, pp. 2706-2717, **2002**.
- [72] A. Oromiehie, H. Ebadi-Dehaghani, and S. Mirbagheri, "Chemical modification of polypropylene by maleic anhydride: Melt grafting, characterization and mechanism," *International Journal of Chemical Engineering and Applications*, vol. 5, p. 117, **2014**.
- [73] F. Berzin, J.-J. Flat, and B. Vergnes, "Grafting of maleic anhydride on polypropylene by reactive extrusion: effect of maleic anhydride and peroxide concentrations on reaction yield and products characteristics," in *Journal of Polymer Engineering* vol. 33, ed. **2013**, p. 673.
- [74] C. Li, Y. Zhang, and Y. Zhang, "Melt grafting of maleic anhydride onto low-density polyethylene/polypropylene blends," *Polymer Testing*, vol. 22, pp. 191-195, 2003/04/01/ **2003**.
- [75] J. P. Lawler and A. Charlesby, "Grafting of acrylic acid onto polyethylene using radiation as initiator," *Radiation Physics and Chemistry (1977)*, vol. 15, pp. 595-602, 1980/01/01/ **1980**.
- [76] C. Cai, Q. Shi, L. Li, L. Zhu, and J. Yin, "Grafting acrylic acid onto polypropylene by reactive extrusion with pre-irradiated PP as initiator," *Radiation Physics and Chemistry*, vol. 77, pp. 370-372, 2008/03/01/ **2008**.
- [77] J. Zhou, W. Yu, and C. Zhou, "Rheokinetic study on homogeneous polymer reactions in melt state under strong flow field," *Polymer*, vol. 50, pp. 4397-4405, 2009/08/26/ 2009.
- [78] W. J. Sichina, "DSC as Problem Solving Tool: Measurement of Percent Crystallinity of Thermoplastics," **2000**.
- [79] M. Bousmina, A. Ait-Kadi, and J. B. Faisant, "Determination of shear rate and viscosity from batch mixer data," *Journal of Rheology*, vol. 43, pp. 415-433, **1999**.
- [80] J.-J. F. a. B. V. Françoise Berzin, "polyeng," *Polymer Engineering*, vol. 33, pp. 673-682, **2013**.
- [81] J.-J. F. Françoise Berzin, Bruno Vergnes, "Grafting of maleic anhydride on polypropylene by reactive extrusion: Effect of maleic anhydride and peroxide

- concentrations on reaction yield and products characteristics," *Journal of Polymer Engineering*, pp. 673-682, 10-4-**2013**.
- [82] C. Guo, L. Zhou, and J. Lv, "Effects of expandable graphite and modified ammonium polyphosphate on the flame-retardant and mechanical properties of wood flour-polypropylene composites," *Polymers & Polymer Composites*, vol. 21, p. 449, **2013**.
- [83] Q. Song, Y. Xia, S. Hu, J. Zhao, and G. Zhang, "Tuning the crystallinity and degradability of PCL by organocatalytic copolymerization with δ -hexalactone," *Polymer*, vol. 102, pp. 248-255, **2016**.
- [84] N. C. Abdul Razak, I. M. Inuwa, A. Hassan, and S. A. Samsudin, "Effects of compatibilizers on mechanical properties of PET/PP blend," *Composite Interfaces*, vol. 20, pp. 507-515, 2013/10/01 **2013**.
- [85] M. Akbari, A. Zadhoush, and M. Haghghat, "PET/PP blending by using PP-g-MA synthesized by solid phase," *Journal of applied polymer science*, vol. 104, pp. 3986-3993, **2007**.